IMPRS astronomy & astrophysics Bonn and Cologne

Multi-frequency linear and circular radio polarization monitoring of jet emission elements in Fermi blazars

Ioannis Myserlis

PhD Advisor: Dr. E. Angelakis

Collaborators:
Dr. L. Fuhrmann, Prof. V. Pavlidou
Dr. A. Kraus, V. Karamanavis, Prof. A. Zensus

Max-Planck Institut für Radioastronomie

Outline

- Polarization production mechanisms in AGN jets
- Polarization as a probe of micro-physics in blazars
- Polarization in the time and frequency domains

Why?

- The F-GAMMA program
- Mueller matrix analysis
- Data reduction progress

How?

- Results

Polarization production mechanisms in AGN jets

Radio emission mechanism:
Incoherent synchrotron radiation

Synchrotron radiation is highly polarized

Radiative transfer effects can alter the polarization characteristics

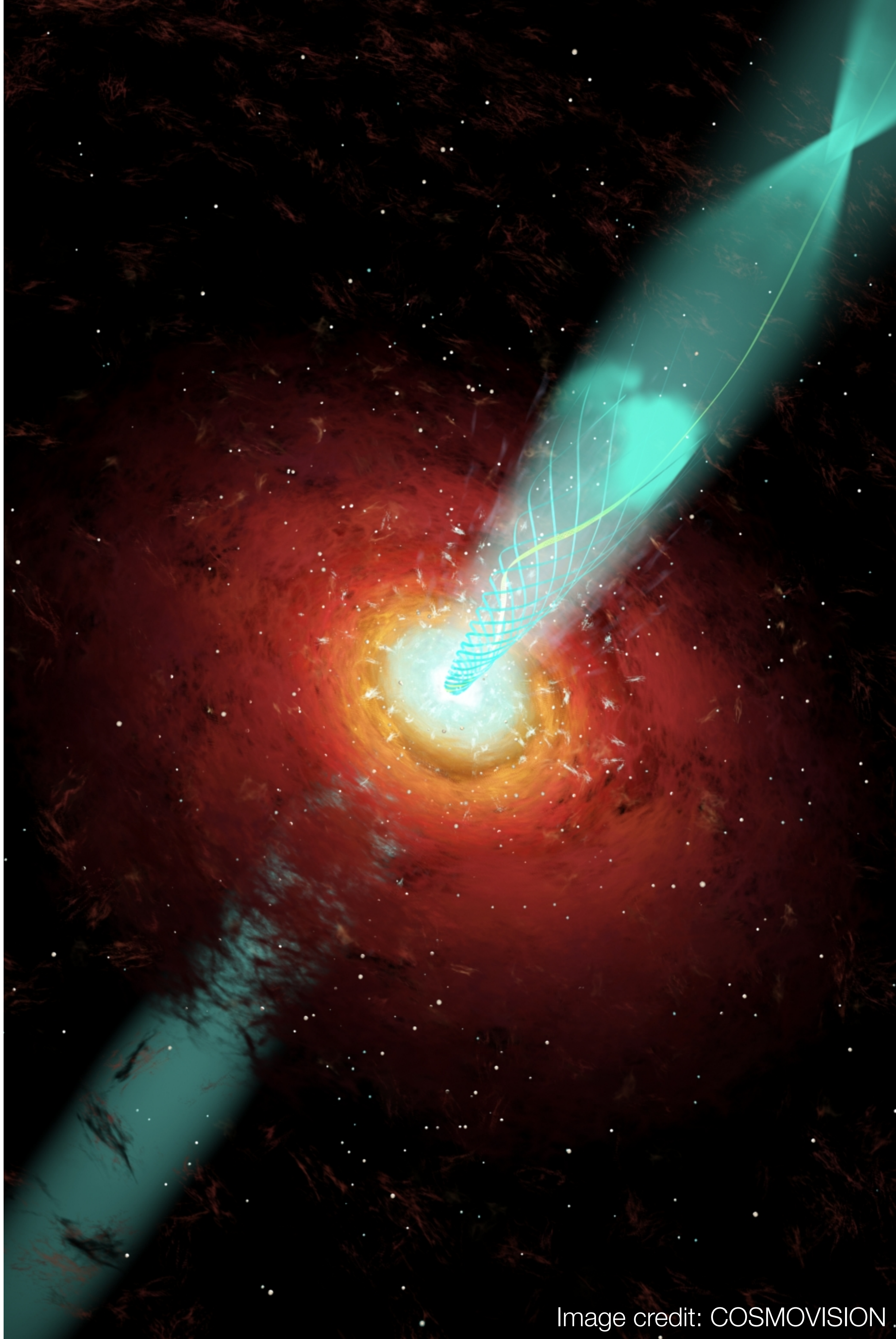

Image credit: COSMOVISION

Polarization production mechanisms in AGN jets

Synchrotron Self Absorbed (SSA) spectrum

$$N(E)dE = \kappa E^{-s} dE \rightarrow S_\nu \propto \nu^{-\frac{s-1}{2}} = \nu^{-a}$$

Canonical value for AGN: $a \approx 0.7$

Self absorbed $S_\nu \propto \nu^{+2.5}$

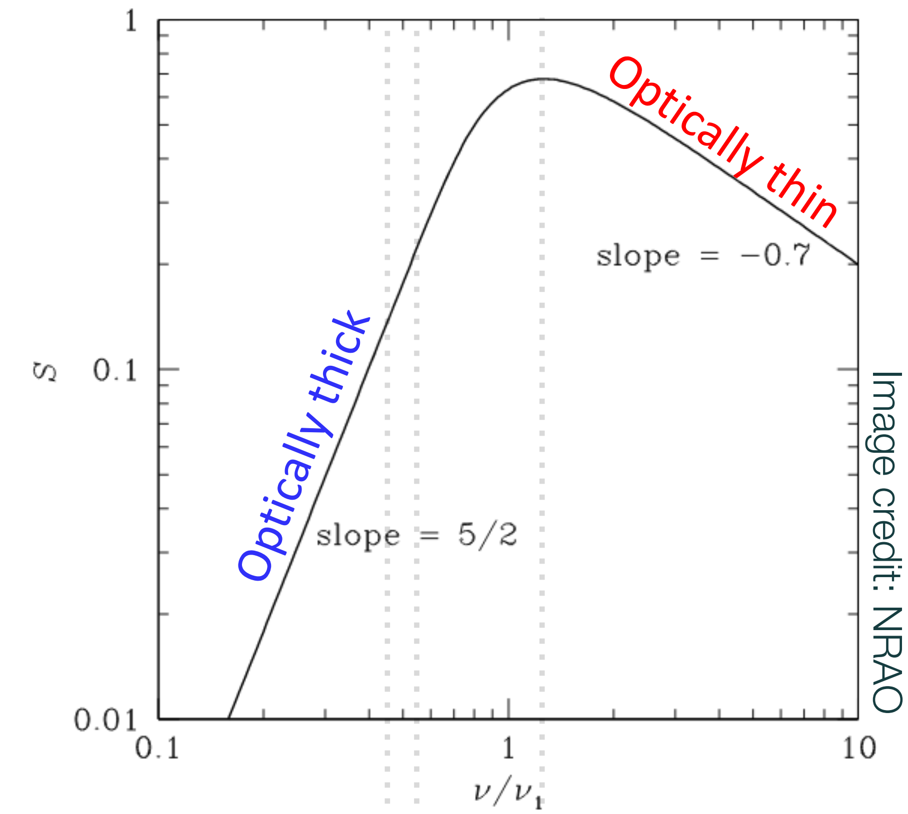

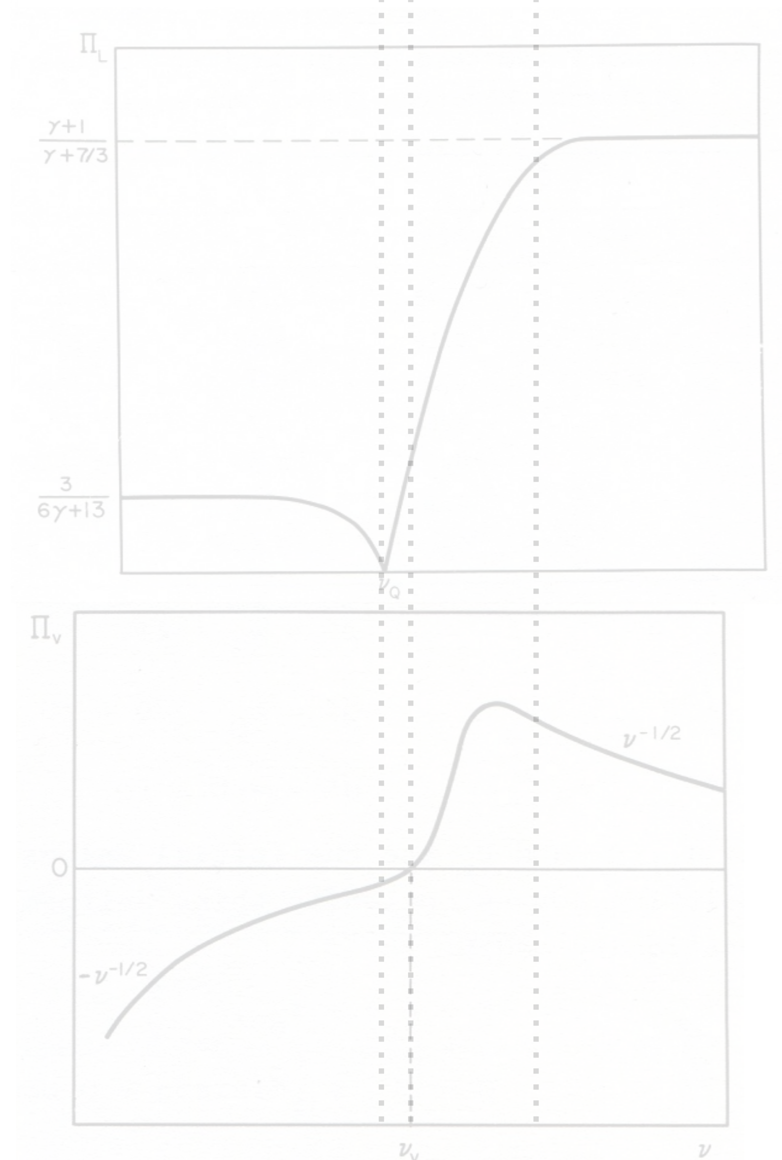

Pacholczyk A.G. (1977)

Polarization production mechanisms in AGN jets

Linear polarization (LP) component of synchrotron sources

- Optically thin

$$m_l = \frac{s+1}{s+\frac{7}{3}} = \frac{a+1}{a+\frac{5}{3}} \approx 72\%$$

Perpendicular to the projected magnetic field

- Optically thick

$$m_l = \frac{3}{6s+13} = \frac{3}{12a+19} \approx 11\%$$

Parallel to the projected magnetic field

Pacholczyk A.G. (1977)

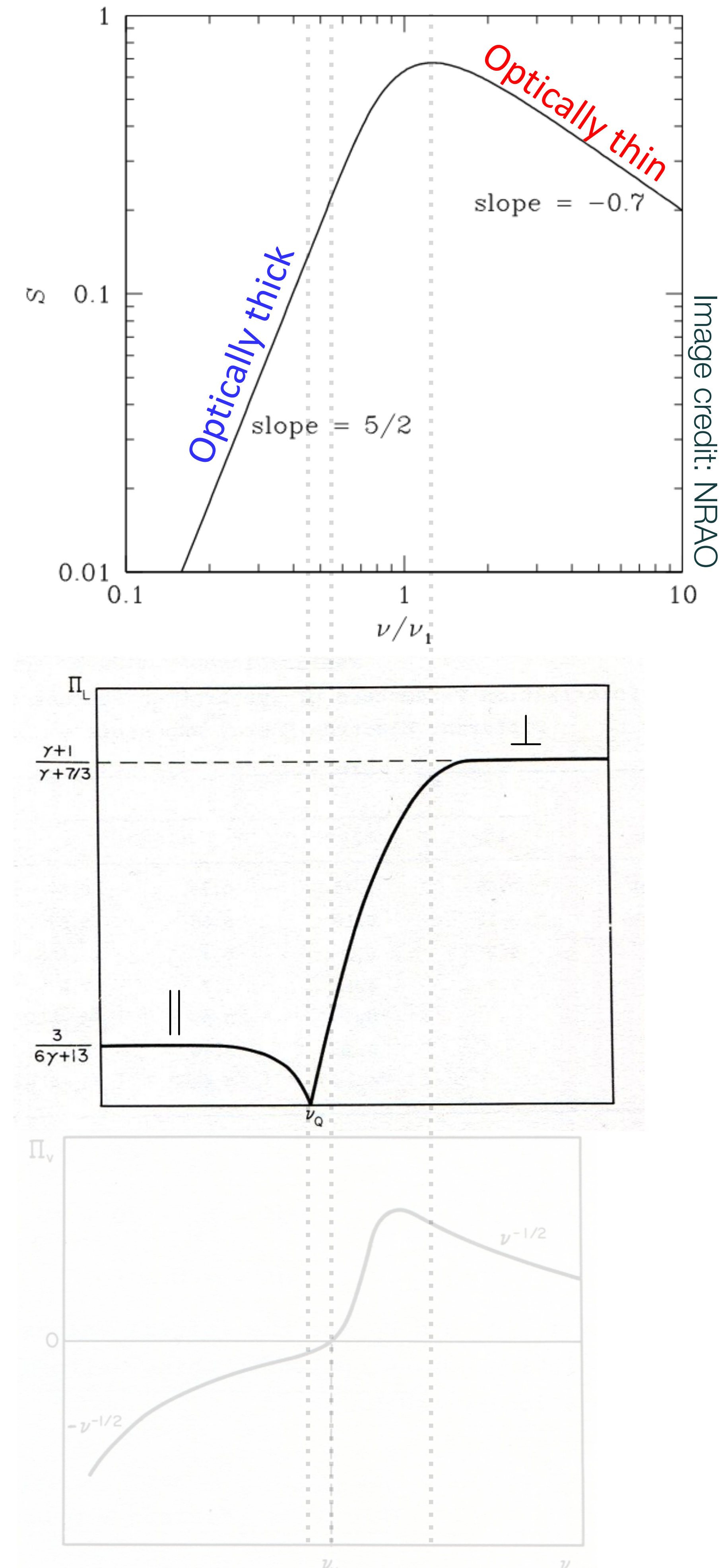

Polarization production mechanisms in AGN jets

Circular polarization (CP) component of synchrotron sources

Low values of circular polarization $m_c \sim 100 \left(\frac{\nu_L}{\nu}\right)^{\frac{1}{2}}$ *(Sciama & Rees, 1967)*

Isotropic pitch angle distribution

- Optically thin $m_c \propto \nu^{-\frac{1}{2}}$
- Optically thick $m_c \propto -\nu^{-\frac{1}{2}}$

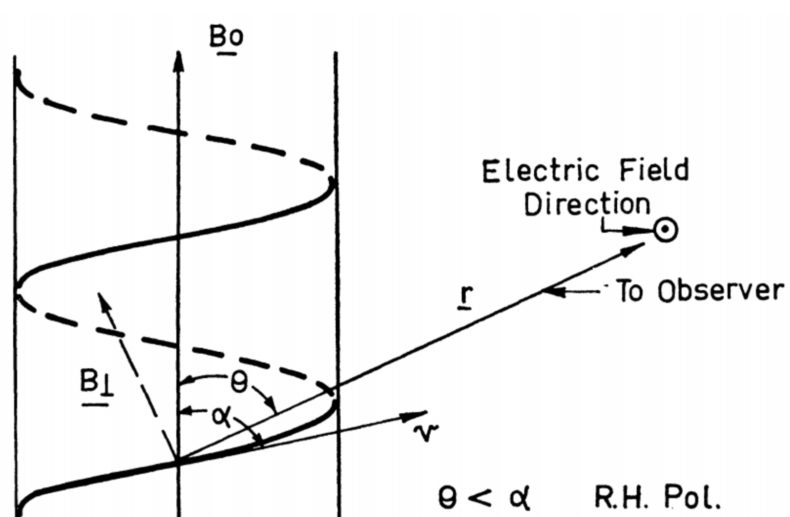

Gardner & Whiteoak (1966)

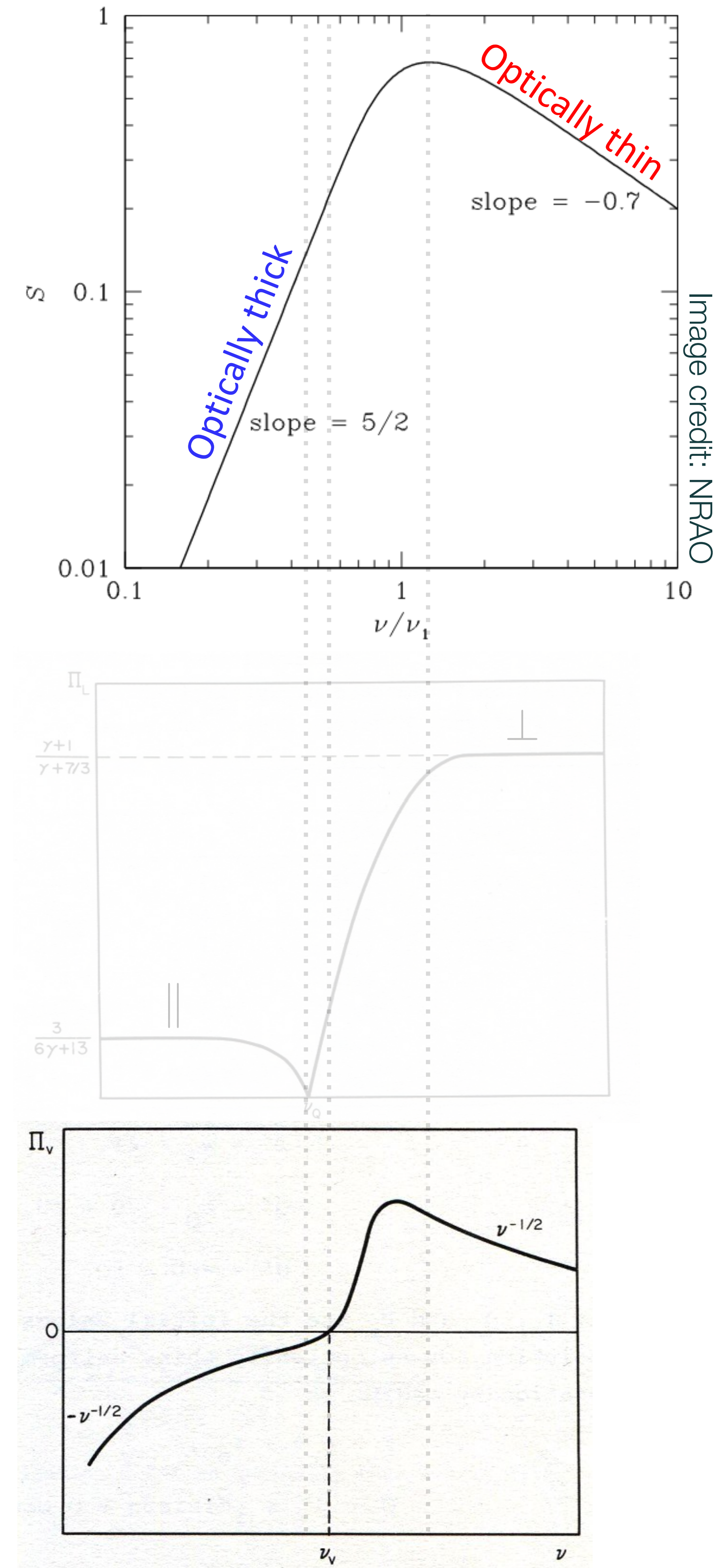

Pacholczyk A.G. (1977)

Polarization production mechanisms in AGN jets

Radiative transfer effects when propagating through magneto-ionic materials

Faraday rotation

LCP and RCP modes with different phase velocities

Faraday depolarization

Rotation decreases as γ increases $\propto \ln(\frac{\gamma}{\gamma^2})$ *(Trubnikov,1958 & Melrose, 1997a)*

$$\Delta\chi = 8.1 \cdot 10^5 \cdot \left(\int_L n_e B_{||} \cos\theta dL\right) \cdot \lambda^2 = RM \cdot \lambda^2 \qquad [rad]$$

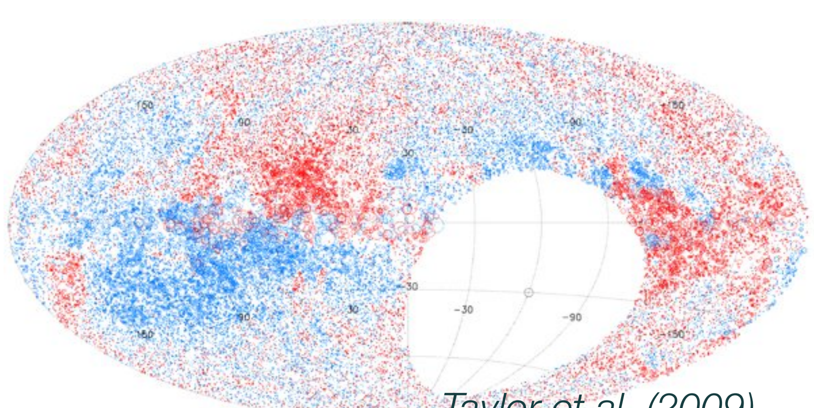

Taylor et al. (2009)

Faraday interconversion / pulsation

Birefringence of the two orthogonal LP modes: $\perp$ & $||$ to the magnetic field

Linear $\longleftrightarrow$ Circular polarization

Relativistic electrons

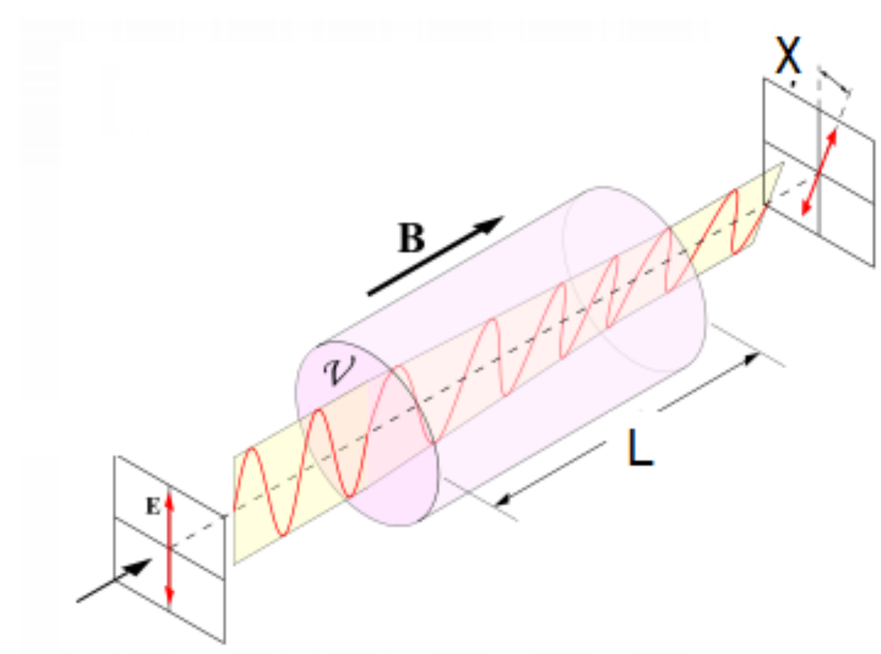

Polarization as a probe of micro-physics in blazars

Synchrotron polarization

Linear polarization is a measure of

$$m_c \sim 100 \left(\frac{\nu_L}{\nu}\right)^{\frac{1}{2}}$$

B-field topology

$$p_c = -\frac{4(\gamma+1)(\gamma+2)}{3\gamma(\gamma+\frac{7}{3})} \frac{\Gamma\left(\frac{3\gamma+4}{12}\right)\Gamma\left(\frac{3\gamma+8}{12}\right)}{\Gamma\left(\frac{3\gamma-1}{12}\right)\Gamma\left(\frac{3\gamma+7}{12}\right)} \times \left(\mathrm{ctg}\,\varphi + \frac{1}{\gamma+2}\frac{1}{Y}\frac{dY}{d\varphi}\right)\left(\frac{B\sin\varphi}{B_\nu}\right)$$

B-field uniformity $\epsilon = \frac{B_0}{B}$

Circular polarization is a measure of

B-field magnitude

B-field uniformity

Pitch angle distribution

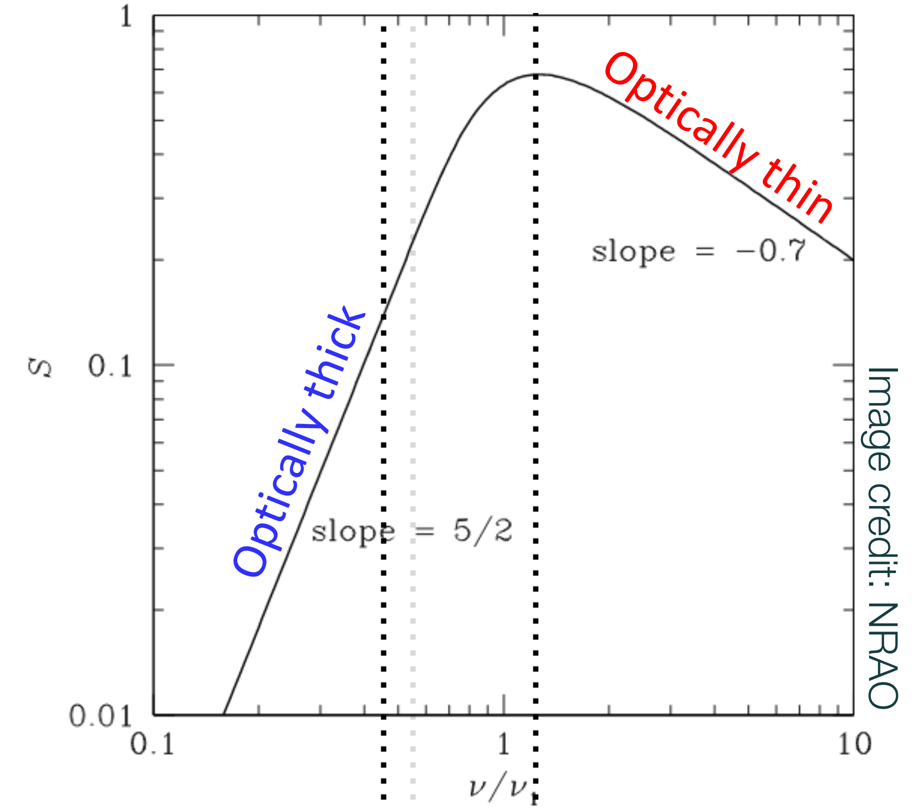

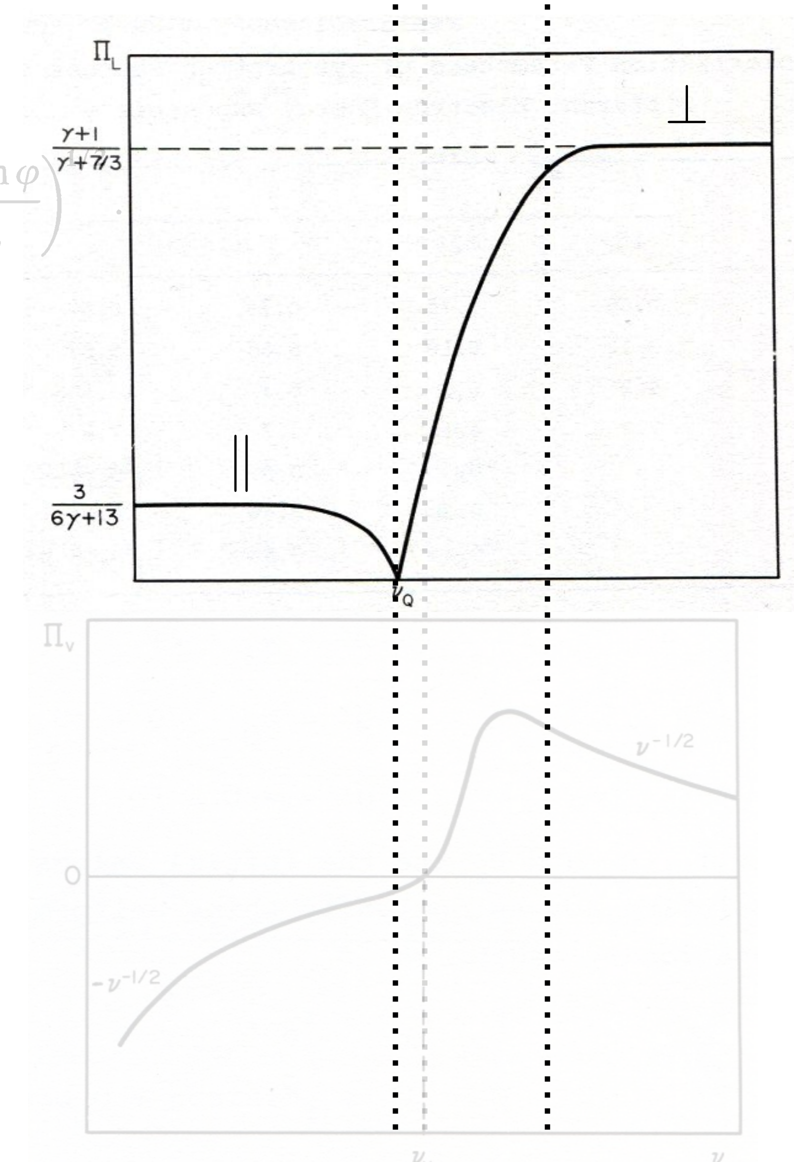

Pacholczyk A.G. (1977)

Gardner & Whiteoak (1966)

Polarization as a probe of micro-physics in blazars

Synchrotron polarization

$$m_c \sim 100 \left(\frac{\nu_L}{\nu}\right)^{\frac{1}{2}}$$

Linear polarization is a measure of

B-field topology

$$p_c = -\frac{4(\gamma+1)(\gamma+2)}{3\gamma\left(\gamma+\frac{7}{3}\right)} \frac{\Gamma\left(\frac{3\gamma+4}{12}\right)\Gamma\left(\frac{3\gamma+8}{12}\right)}{\Gamma\left(\frac{3\gamma-1}{12}\right)\Gamma\left(\frac{3\gamma+7}{12}\right)} \times \times \left(\mathrm{ctg}\,\varphi + \frac{1}{\gamma+2}\frac{1}{Y}\frac{\mathrm{d}Y}{\mathrm{d}\varphi}\right)\left(\frac{B\sin\varphi}{B_\nu}\right)^{1/2}.$$

B-field uniformity $\epsilon = \frac{B_0}{B}$

Circular polarization is a measure of

B-field magnitude

B-field uniformity

Pitch angle distribution

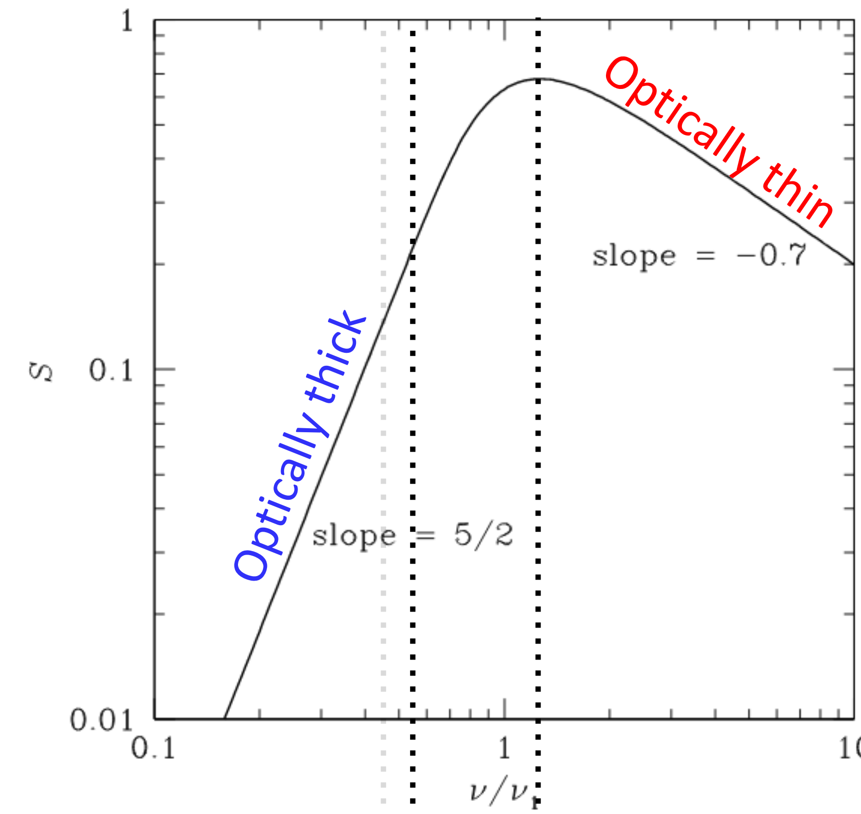

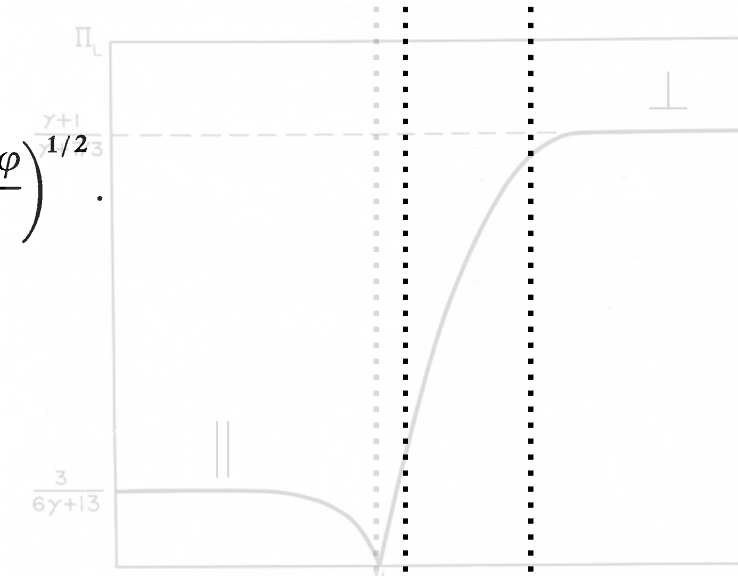

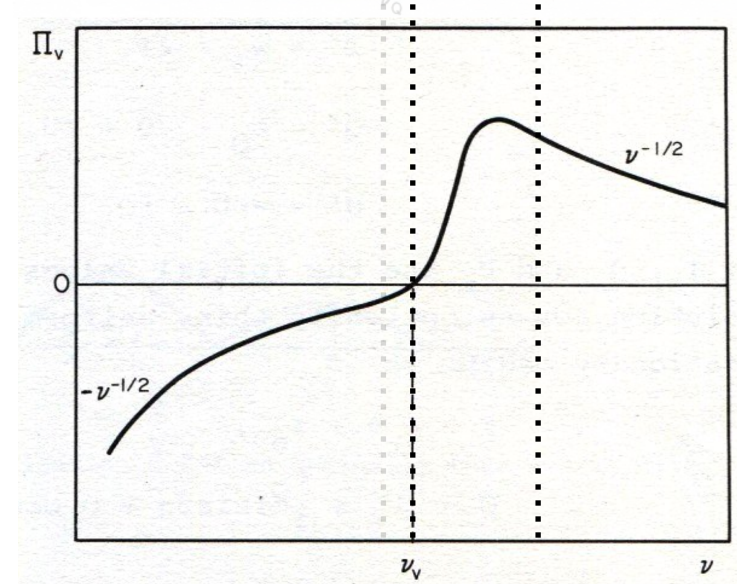

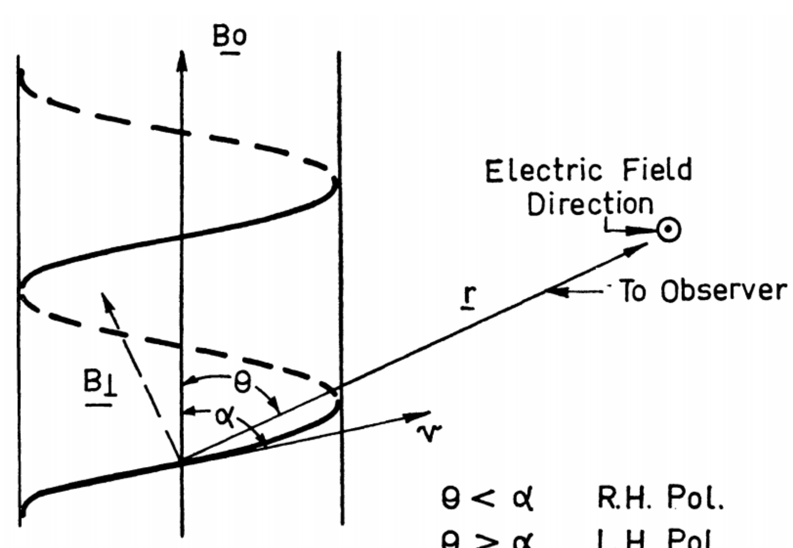

Gardner & Whiteoak (1966)

Pacholczyk A.G. (1977)

Polarization as a probe of micro-physics in blazars

Radiative transfer coefficients through the jet plasma

Faraday rotation (FR) and conversion (FC) coefficients

Diversity between different plasma states, e.g. cold or relativistic

LP/CP degrees ratio is a measure of the FR/FC coefficients ratio

Investigate the state of the jet plasma

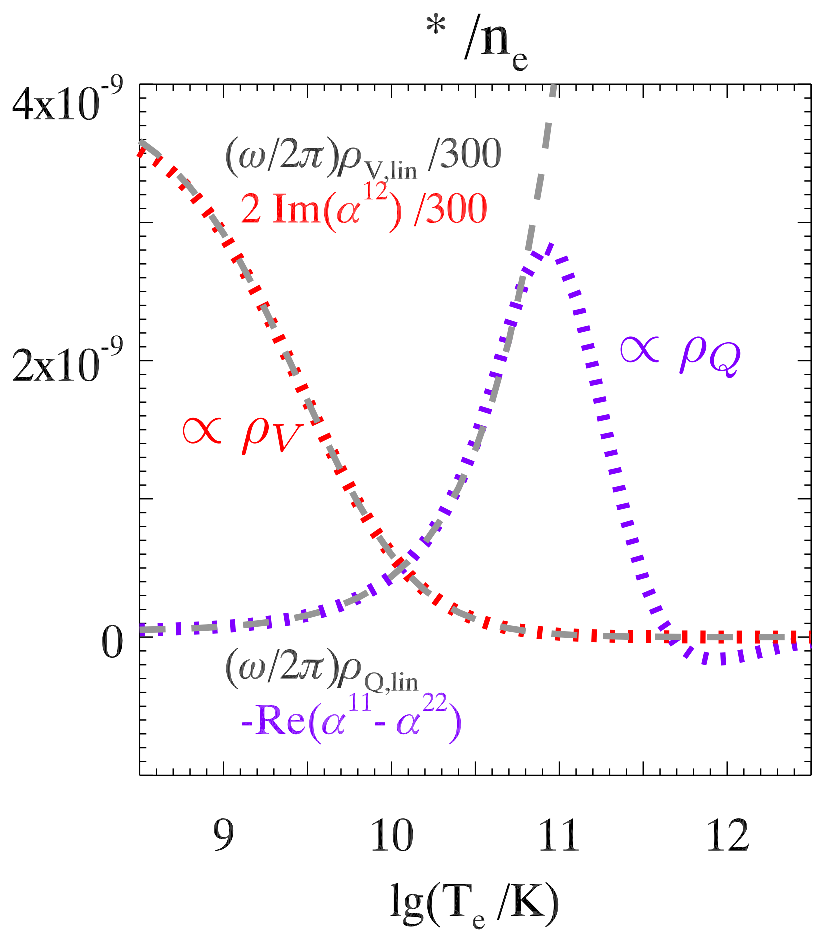

Huang & Shcherbakov (2011)

$$\frac{d\boldsymbol{S}}{ds} = \begin{pmatrix} \varepsilon_I \\ \varepsilon_Q \\ 0 \\ \varepsilon_V \end{pmatrix} - \begin{pmatrix} \eta_I & \eta_Q & 0 & \eta_V \\ \eta_Q & \eta_I & \rho_V & 0 \\ 0 & -\rho_V & \eta_I & \rho_Q \\ \eta_V & 0 & -\rho_Q & \eta_I \end{pmatrix} \boldsymbol{S}$$

Polarization in the time and frequency domains

Synchrotron polarization characteristics have an analytical description in the frequency domain

Blazar variability:
Propagation of high energy SED synchrotron components through the observed bandpass *(Marscher & Gear 1985)*

Multi-band monitoring to trace the evolution of the physical characteristics

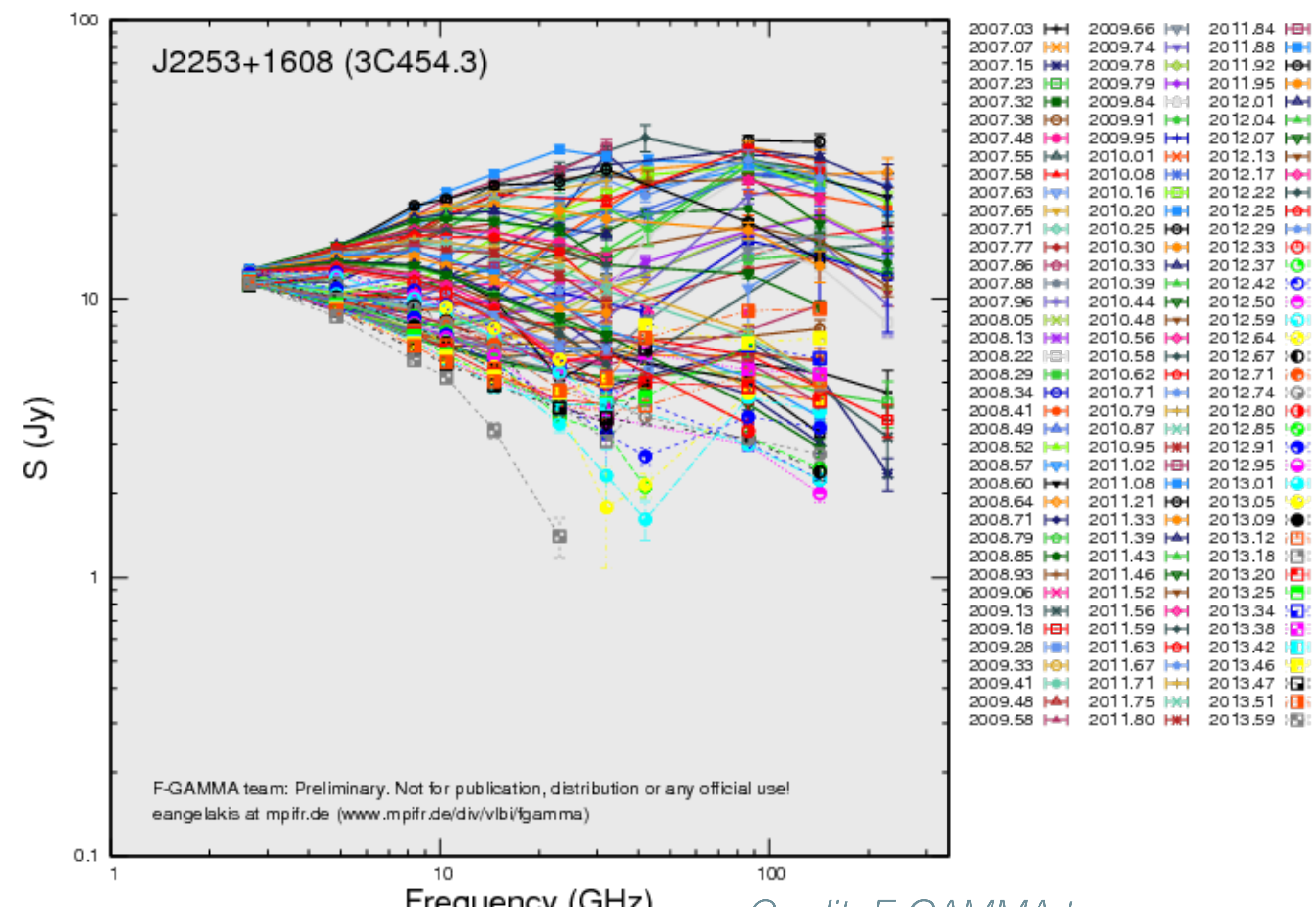

Credit: F-GAMMA team

Polarization in the time and frequency domains

Analytic description in the frequency domain

Both LP and CP decrease to 0% close to $\nu_m \rightarrow \tau = 1$

LP: $\nu_Q \approx 0.44\nu_m \rightarrow \tau \approx 7$

CP: $\nu_V \approx 0.49\nu_m \rightarrow \tau \approx 5$

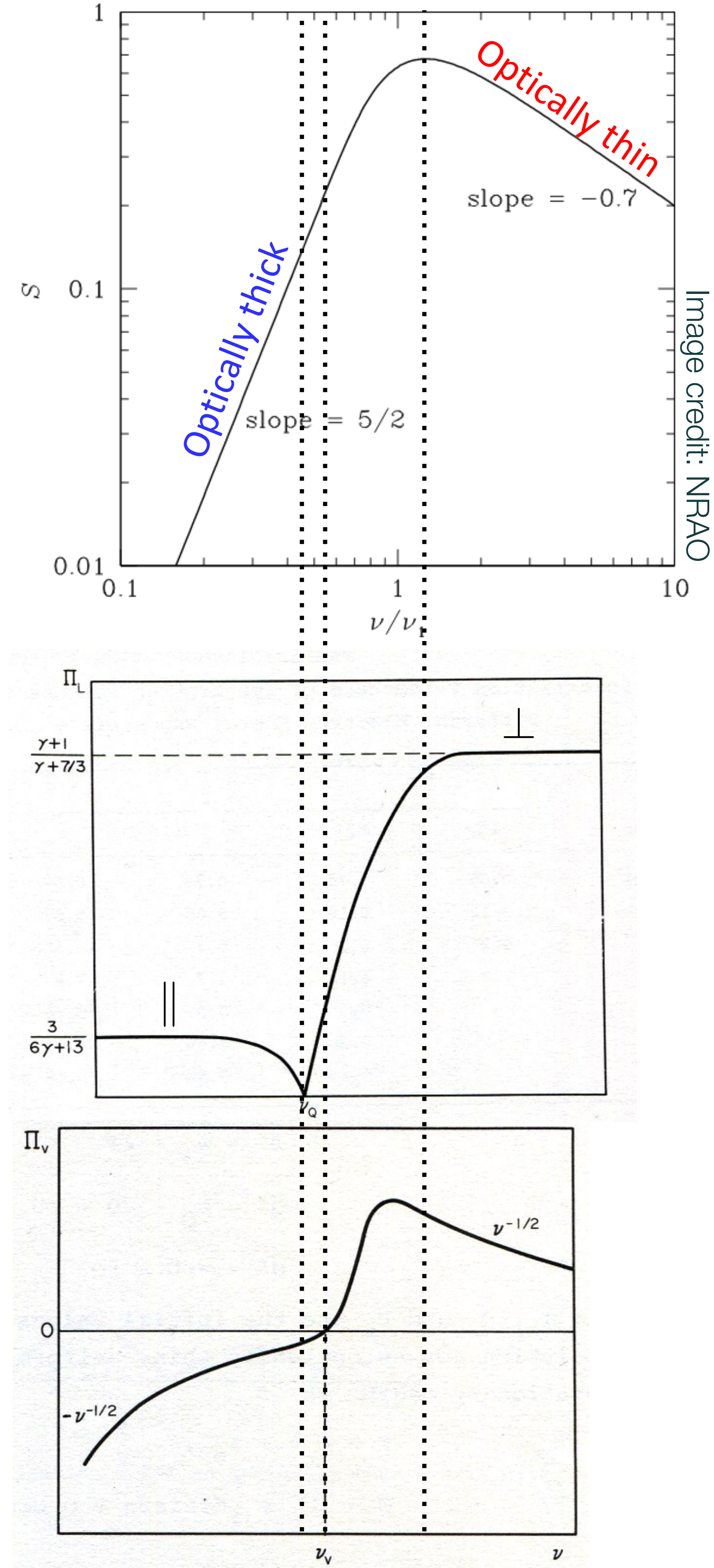

Pacholczyk A.G. (1977)

Polarization in the time and frequency domains

Testing variability models (e.g. shock-in-jet model)

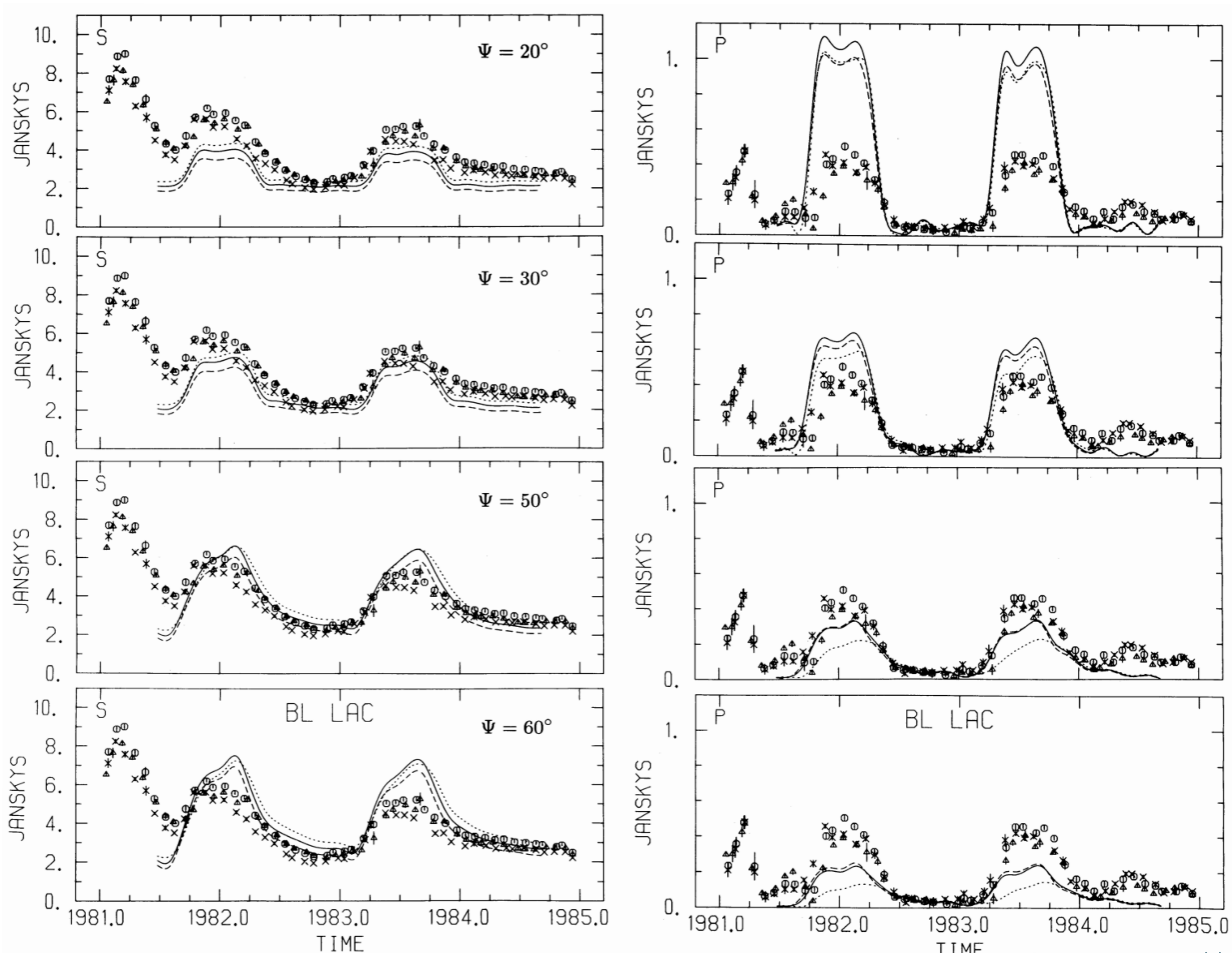

Hughes, Aller,& Aller, 1989

Polarization in the time and frequency domains

Polarization Rotator Events (angle swings)

Geometrical swing

- Emission element on helical path
- Arbitrary magnitude

Radiative "swing"

- Emission element expansion
- Optical depth evolution
- LP drops to 0% and gets to optically thin/thick values
- CP drops to 0% and changes handedness
- Exactly 90 degrees

The mechanisms can operate simultaneously

Radiative "swings" can only be studied at low radio frequencies

Geometrical

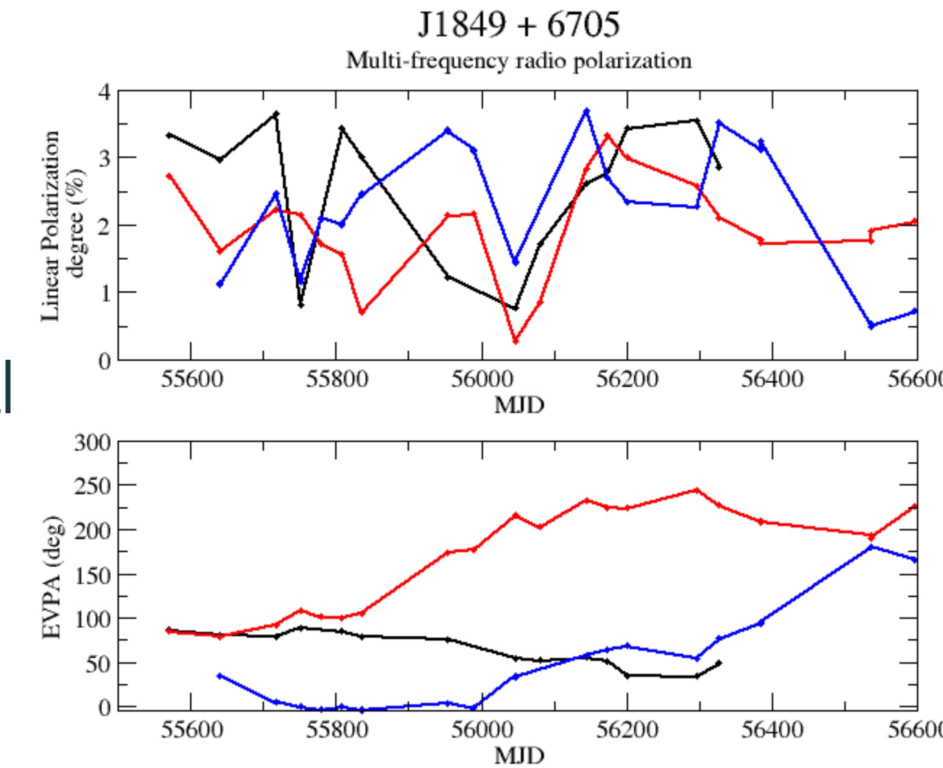

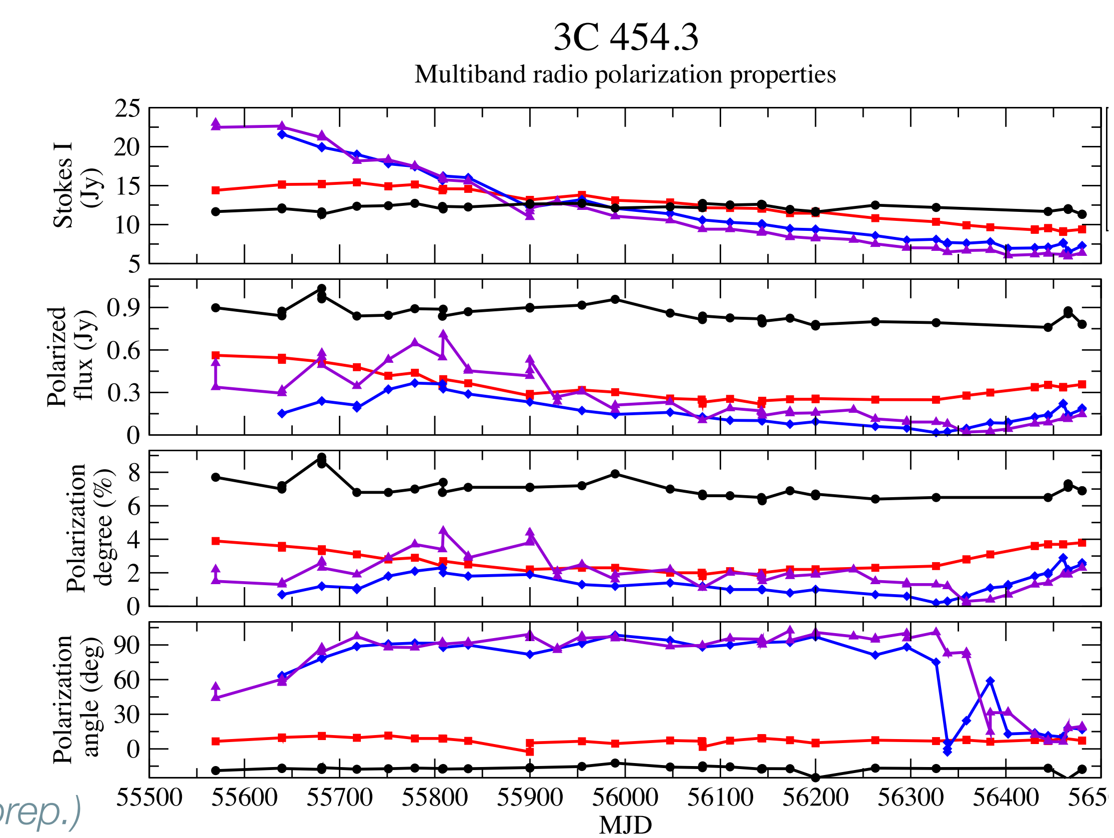

Radiative

Myserlis, Angelakis et al. (in prep.)

The F-GAMMA program

Multifrequency monthly monitoring of 60 γ-ray blazars

- Flux density variability
- Spectral evolution
- Polarization variability

Main facilities

- **100m Effelsberg telescope (Germany)**
  - **2.64, 4.85, 8.35, 10.45, 14.60, 23.05,** 32.00, **42.90 GHz**
- 30m Pico Veleta IRAM (Spain)
  - 88.24, 142.33, 228.39 GHz
- 12m APEX
  - 345 GHz

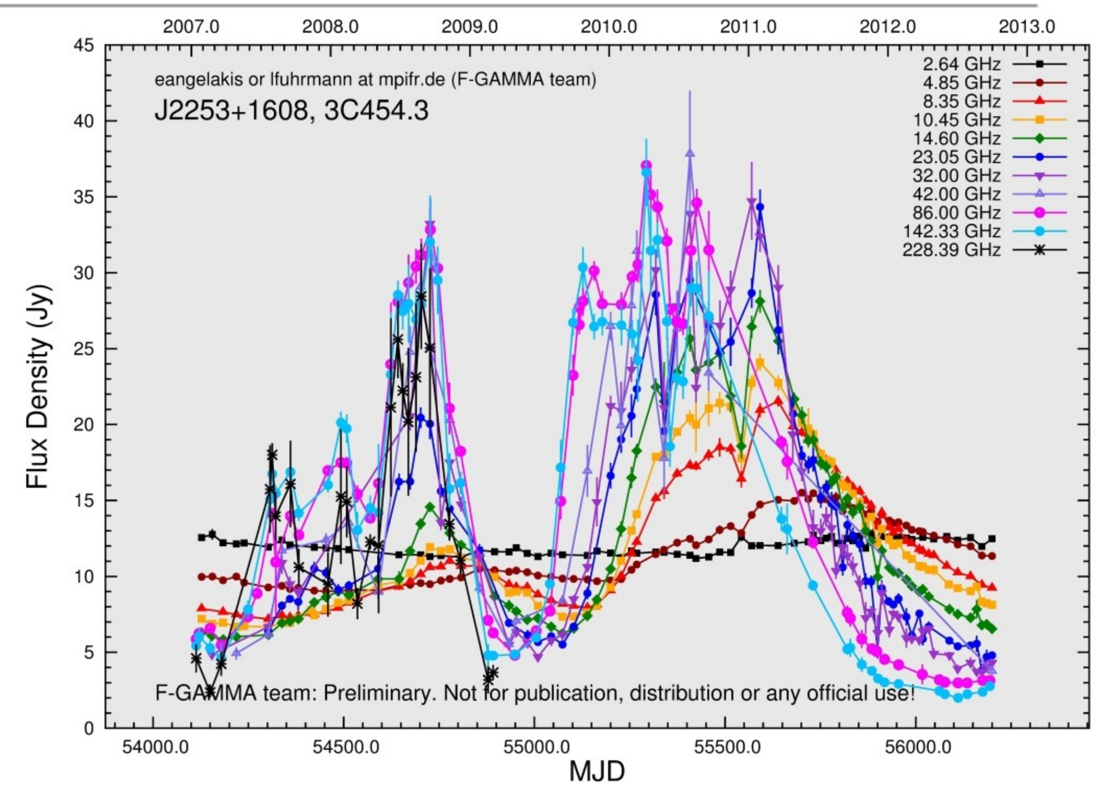

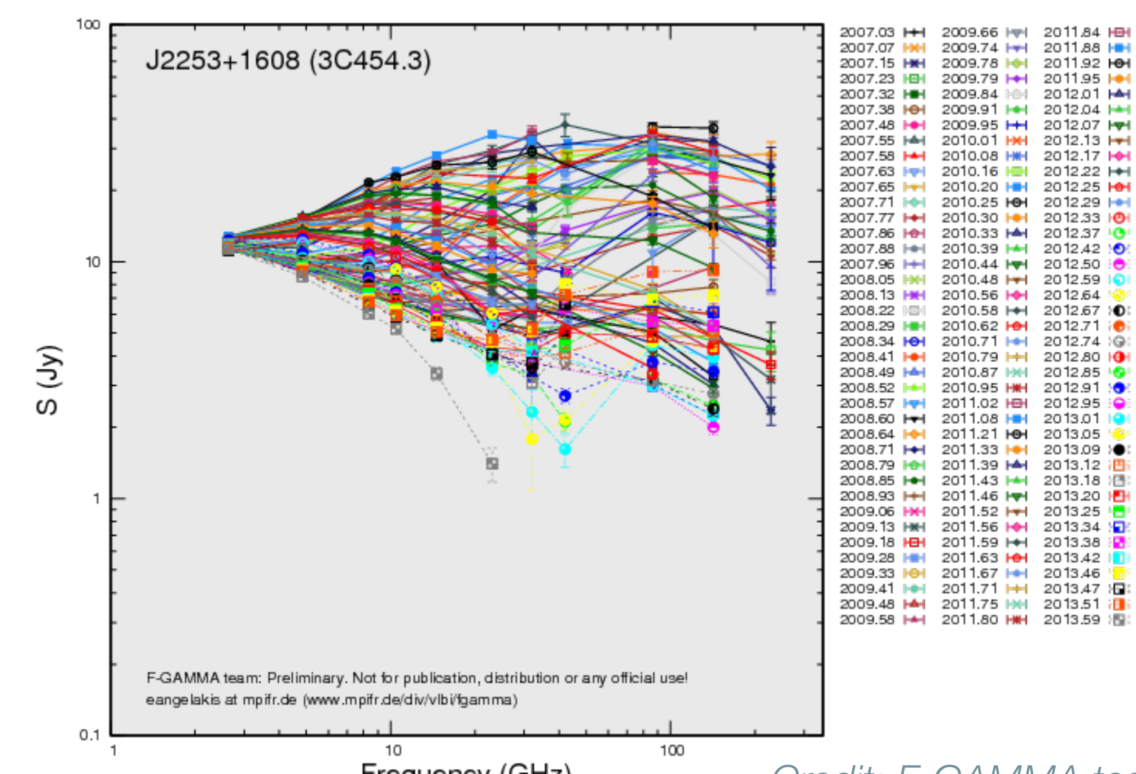

Credit: F-GAMMA team

The F-GAMMA program

4.85 GHz

LP: 75% of the sample $(\widetilde{m}_l = 3.1\%)$

CP: 2% of the sample $(\widetilde{m}_c = 0.4\%)$

10.45 GHz

LP: 39% of the sample $(\widetilde{m}_l = 3.6\%)$

CP: 5% of the sample $(\widetilde{m}_c = 0.4\%)$

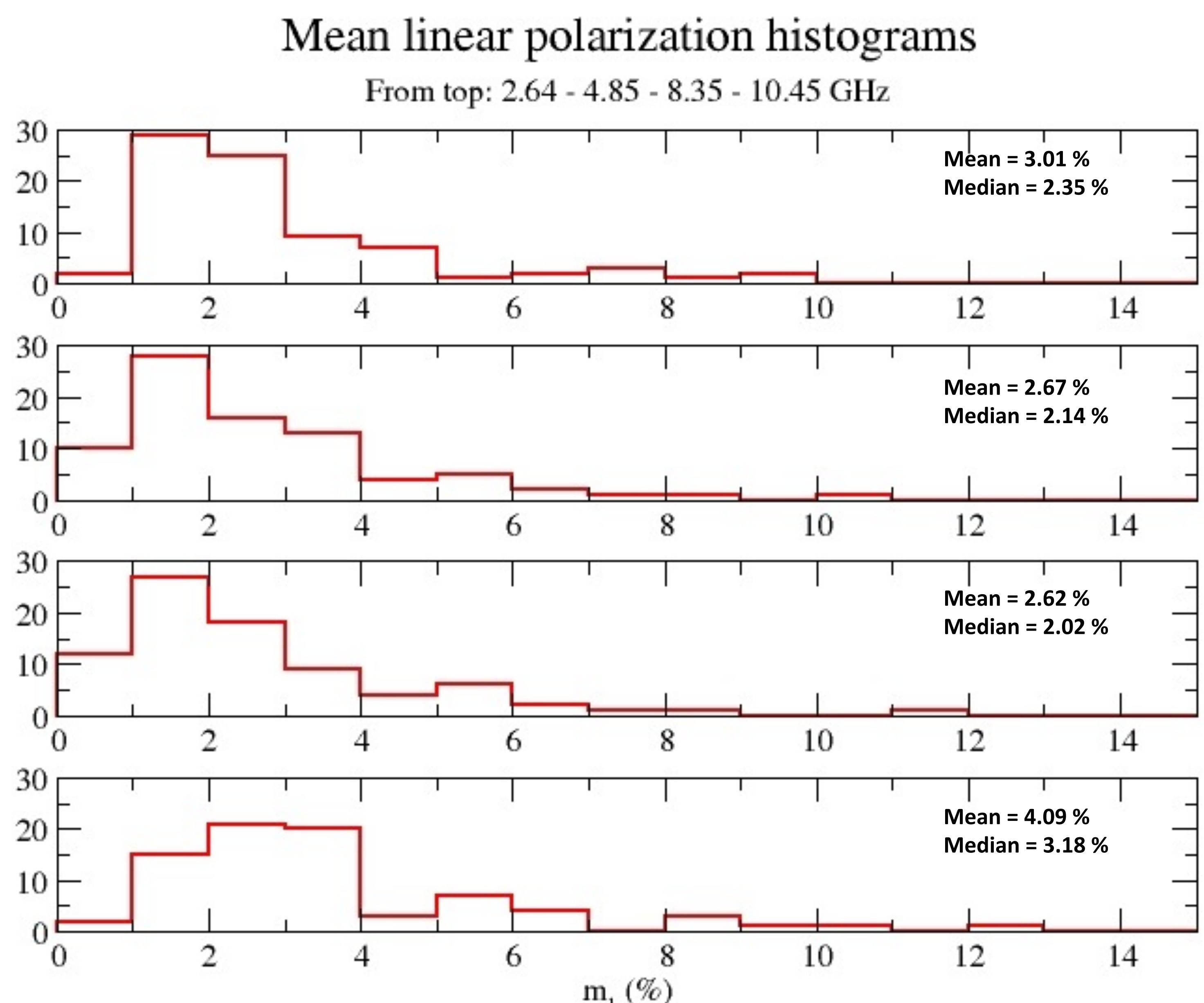

Myserlis, Angelakis et al. (in prep.)

Mueller matrix analysis

$$\begin{pmatrix} I_{obs} \\ Q_{obs} \\ U_{obs} \\ V_{obs} \end{pmatrix} = \begin{pmatrix} m_{11} & m_{12} & m_{13} & m_{14} \\ m_{21} & m_{22} & m_{23} & m_{24} \\ m_{31} & m_{32} & m_{33} & m_{34} \\ m_{41} & m_{42} & m_{43} & m_{44} \end{pmatrix} \cdot \begin{pmatrix} I_{real} \\ Q_{real} \\ U_{real} \\ V_{real} \end{pmatrix}$$

$$\begin{aligned} I_{obs} &= m_{11} \cdot I_{real} + m_{12} \cdot Q_{real} + m_{13} \cdot U_{real} + m_{14} \cdot V_{real} \\ Q_{obs} &= m_{21} \cdot I_{real} + m_{22} \cdot Q_{real} + m_{23} \cdot U_{real} + m_{24} \cdot V_{real} \\ U_{obs} &= m_{31} \cdot I_{real} + m_{32} \cdot Q_{real} + m_{33} \cdot U_{real} + m_{34} \cdot V_{real} \\ V_{obs} &= m_{41} \cdot I_{real} + m_{42} \cdot Q_{real} + m_{43} \cdot U_{real} + m_{44} \cdot V_{real} \end{aligned}$$

Method

1. Observe sources with known polarization characteristics
2. Solve the system of equations [1] by fitting our measurements
3. Apply the instrumental polarization correction to our target sources

Full Stokes calibration problems

- Lack of CP calibrators
- Circularly polarized feeds

$$\begin{aligned} I &= |E_l|^2 + |E_r|^2, \\ Q &= 2\mathrm{Re}(E_l^* E_r), \\ U &= -2\mathrm{Im}(E_l^* E_r), \\ V &= |E_l|^2 - |E_r|^2. \end{aligned}$$

Mueller matrix analysis

$$\begin{pmatrix} I_{obs} \\ Q_{obs} \\ U_{obs} \\ V_{obs} \end{pmatrix} = \begin{pmatrix} m_{11} & m_{12} & m_{13} & m_{14} \\ m_{21} & m_{22} & m_{23} & m_{24} \\ m_{31} & m_{32} & m_{33} & m_{34} \\ m_{41} & m_{42} & m_{43} & m_{44} \end{pmatrix} \cdot \begin{pmatrix} I_{real} \\ Q_{real} \\ U_{real} \\ V_{real} \end{pmatrix}$$

$$\begin{aligned} I_{obs} &= m_{11} \cdot I_{real} + m_{12} \cdot Q_{real} + m_{13} \cdot U_{real} + m_{14} \cdot V_{real} \\ Q_{obs} &= m_{21} \cdot I_{real} + m_{22} \cdot Q_{real} + m_{23} \cdot U_{real} + m_{24} \cdot V_{real} \\ U_{obs} &= m_{31} \cdot I_{real} + m_{32} \cdot Q_{real} + m_{33} \cdot U_{real} + m_{34} \cdot V_{real} \\ V_{obs} &= m_{41} \cdot I_{real} + m_{42} \cdot Q_{real} + m_{43} \cdot U_{real} + m_{44} \cdot V_{real} \end{aligned}$$

Method

1. Observe sources with known polarization characteristics
2. Solve the system of equations [1] by fitting our measurements
3. Apply the instrumental polarization correction to our target sources

Full Stokes calibration problems

Lack of CP calibrators

Circularly polarized feeds

$$\begin{aligned} I &= |E_l|^2 + |E_r|^2, \\ Q &= 2\mathrm{Re}(E_l^* E_r), \\ U &= -2\mathrm{Im}(E_l^* E_r), \\ V &= |E_l|^2 - |E_r|^2. \end{aligned}$$

Mueller matrix analysis

CP calibration: relative gain (LCP/RCP) correction

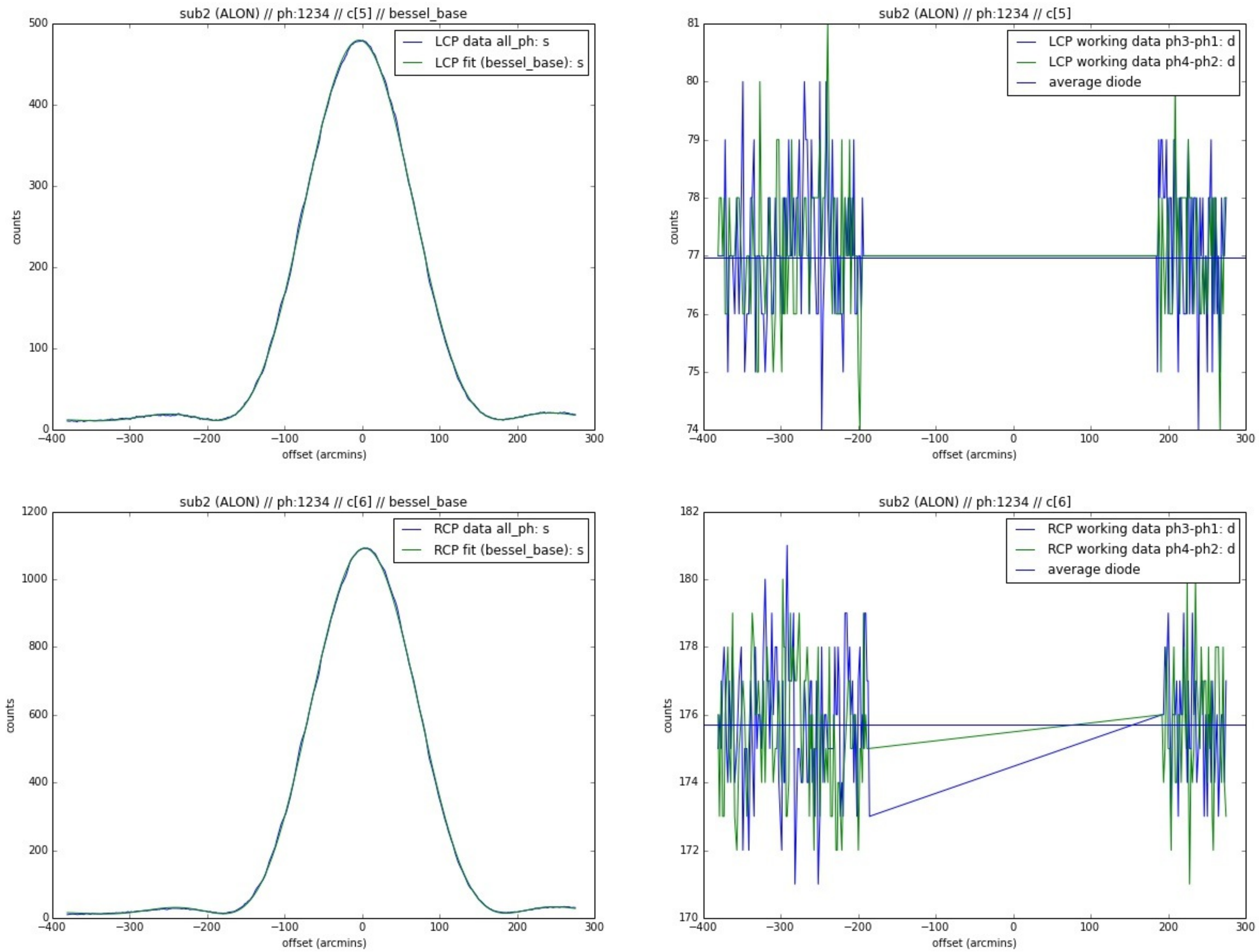

Myserlis, Angelakis et al. (in prep.)

Data reduction progress

Since January 2011

4 frequencies

LP & CP flux

LP & CP degree

EVPA

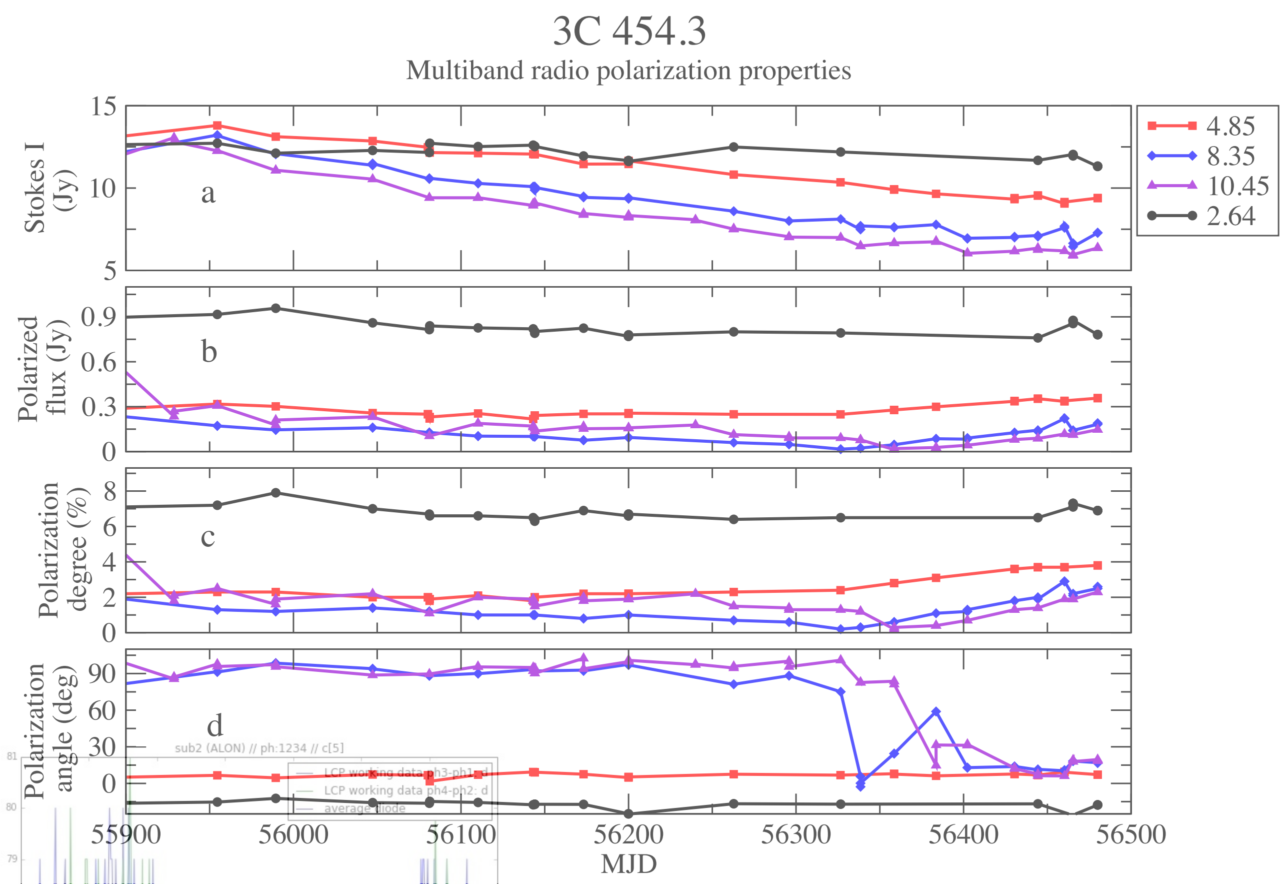

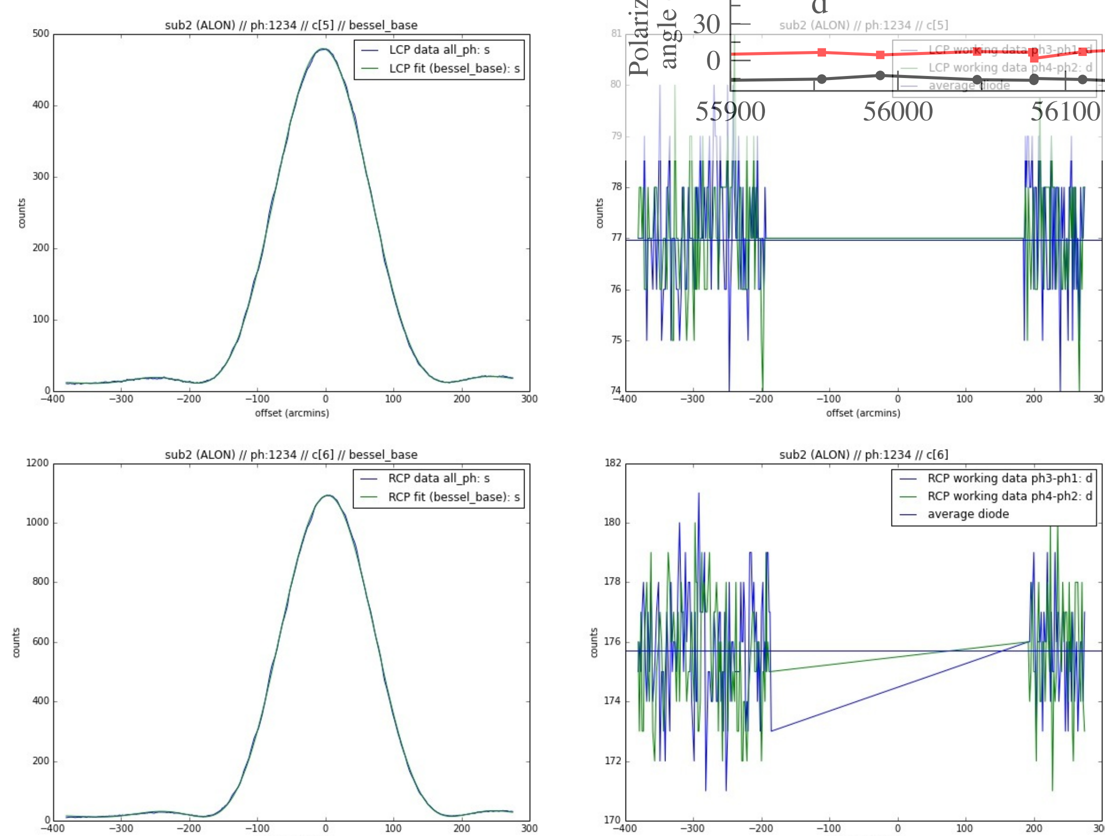

Myserlis, Angelakis et al. (in prep.)

Results

circular polarization calibrator candidates

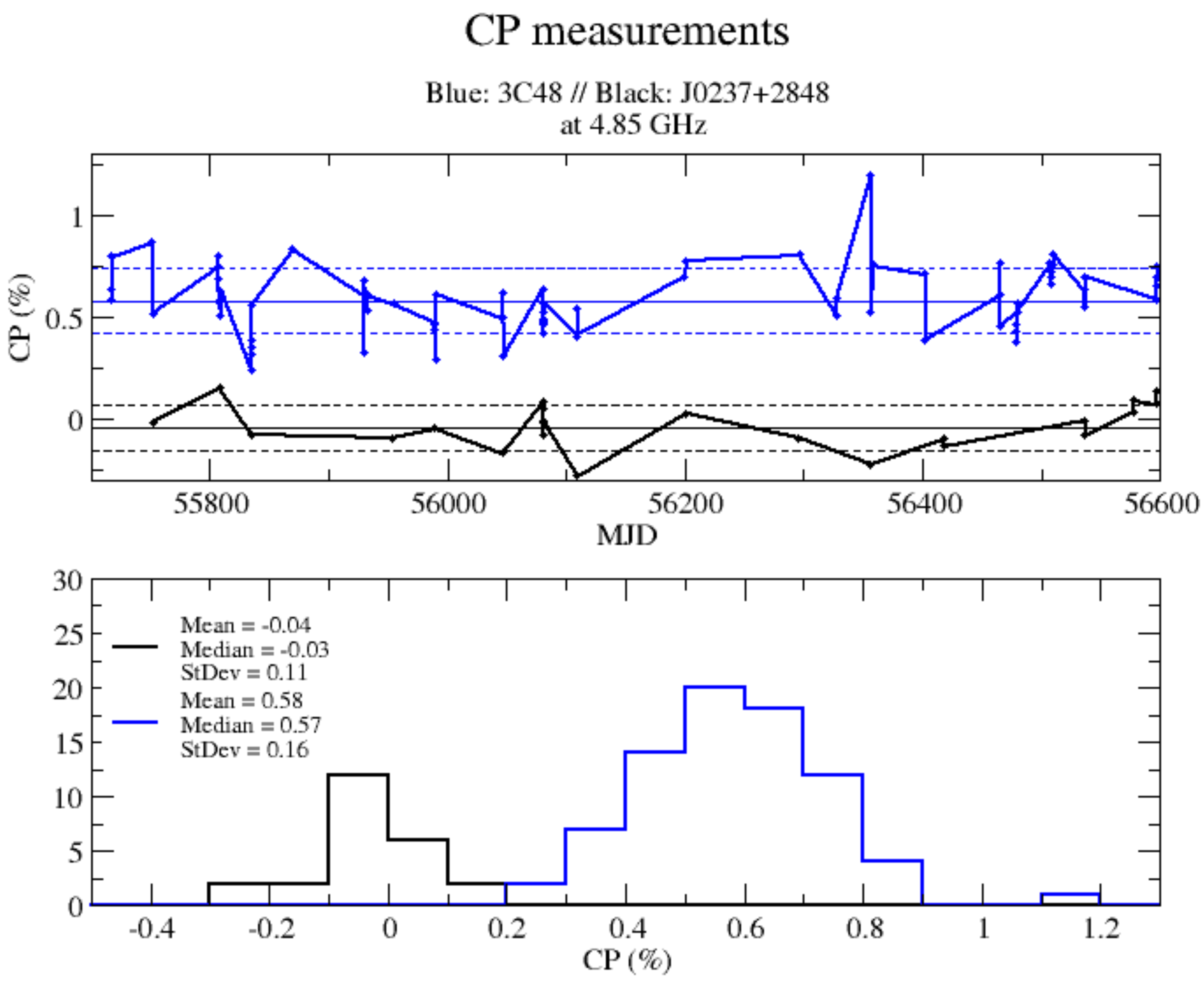

Myserlis, Angelakis et al. (in prep.)

Results

B-field estimation using CP measurements

Assuming intrinsic CP

$$m_c \sim 100 \left(\frac{\nu_L}{\nu}\right)^{\frac{1}{2}}$$

3C48:

CP = 0.58 %
B = 58mG (electron plasma)

Equipartition:

~10 - 100mG
(O'Sullivan & Gabuzda, 2008)

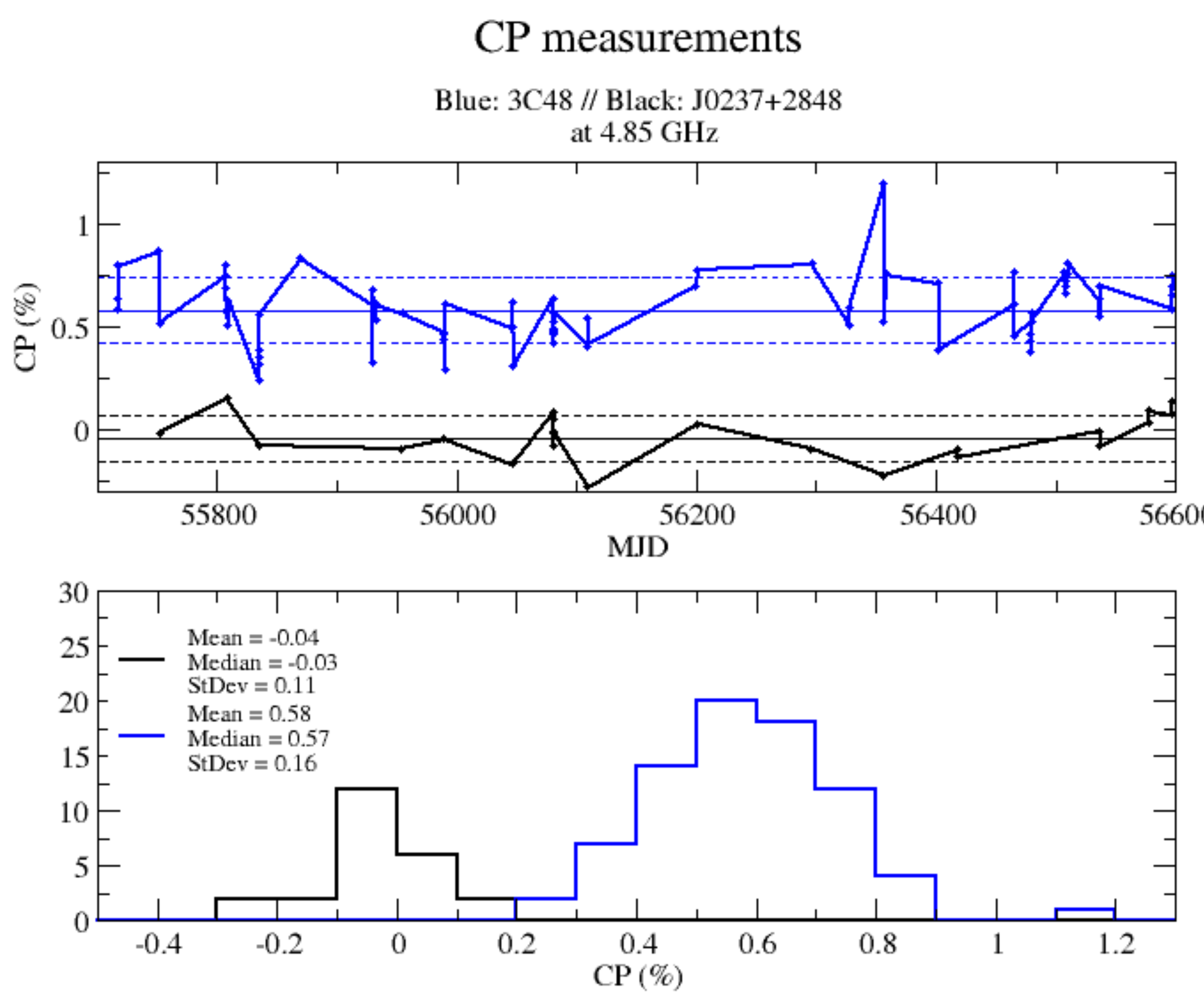

Myserlis, Angelakis et al. (in prep.)

Results

B-field topology

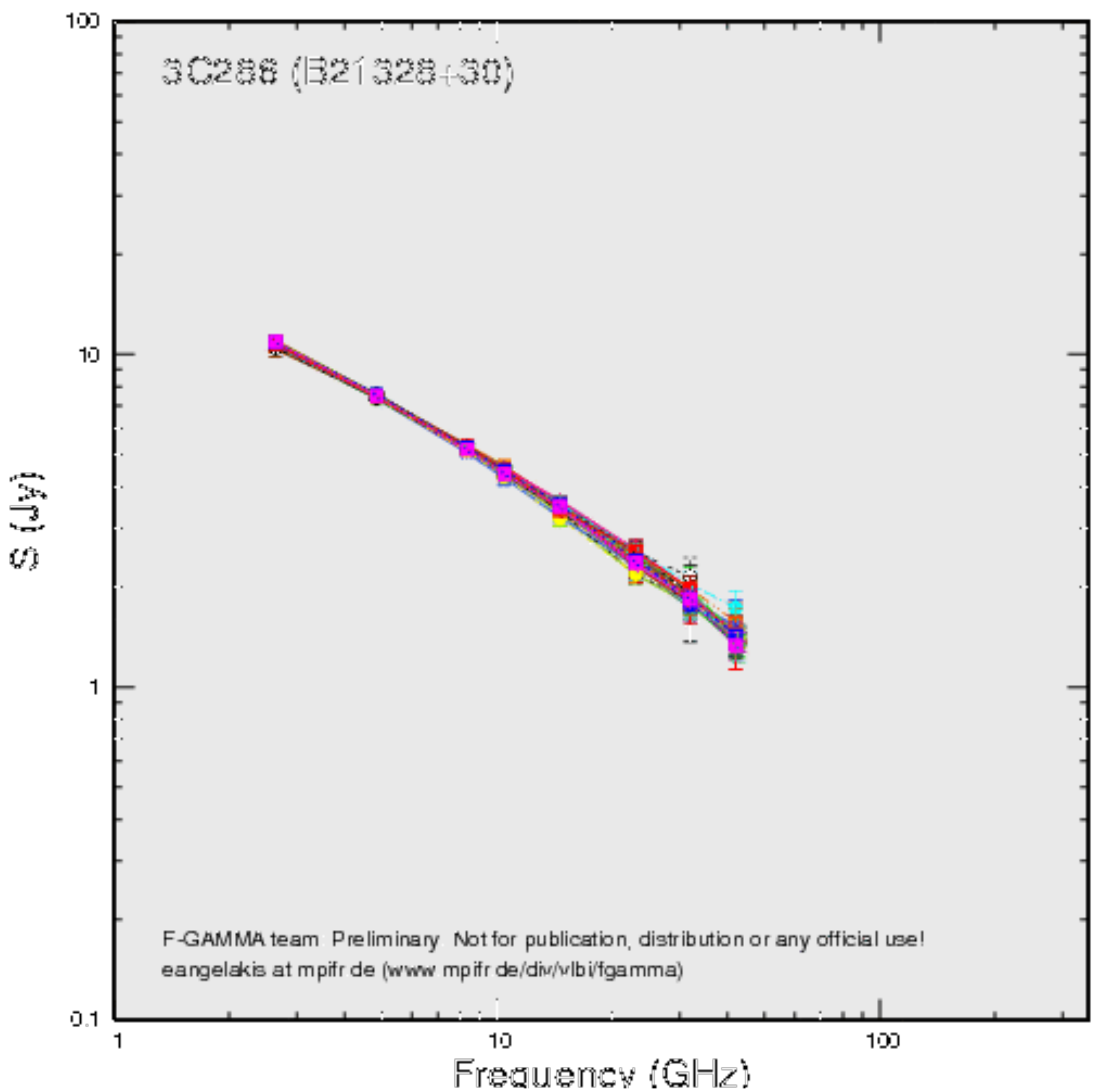

Credit: F-GAMMA team

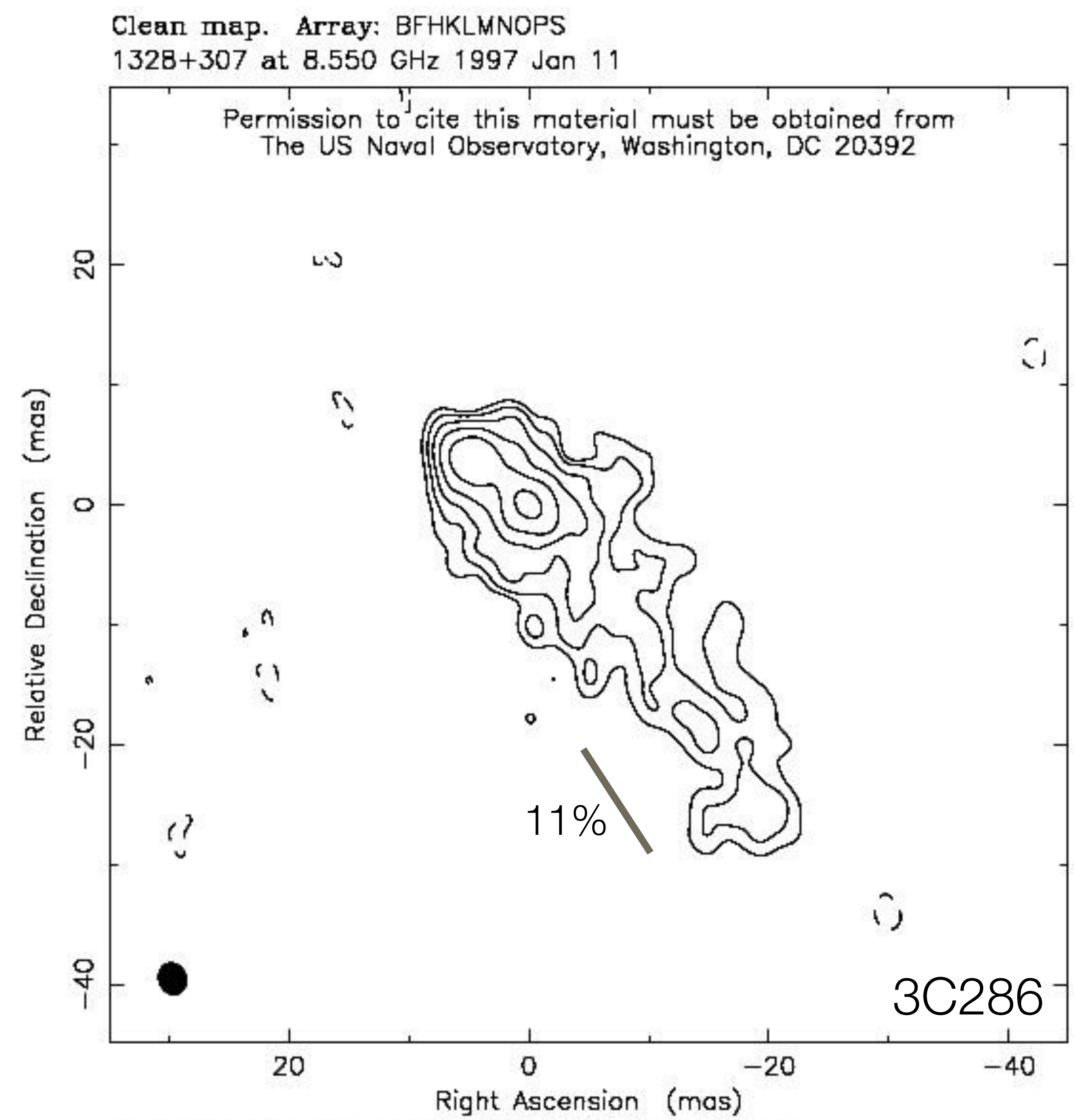

Results

B-field topology

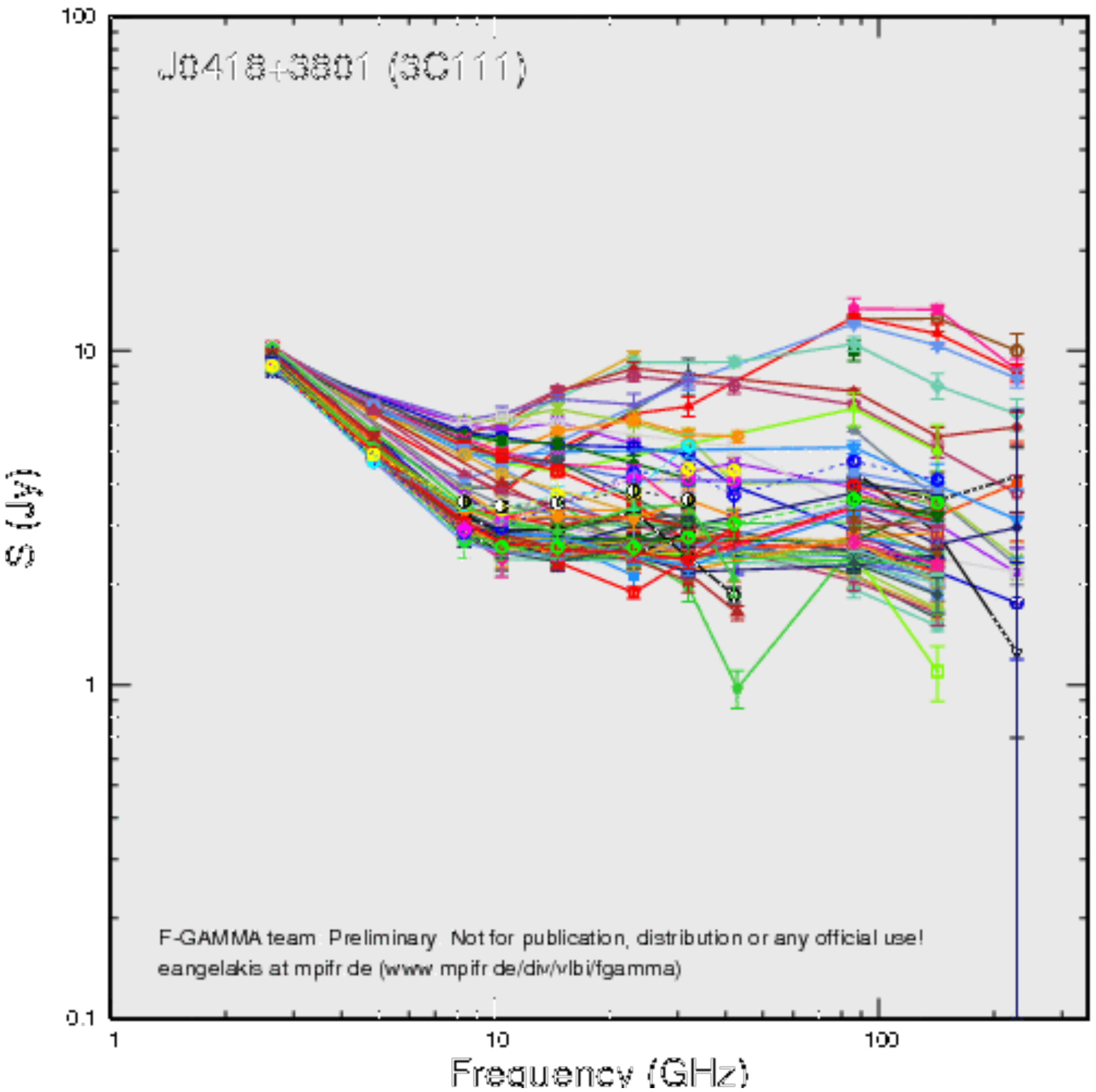

Credit: F-GAMMA team

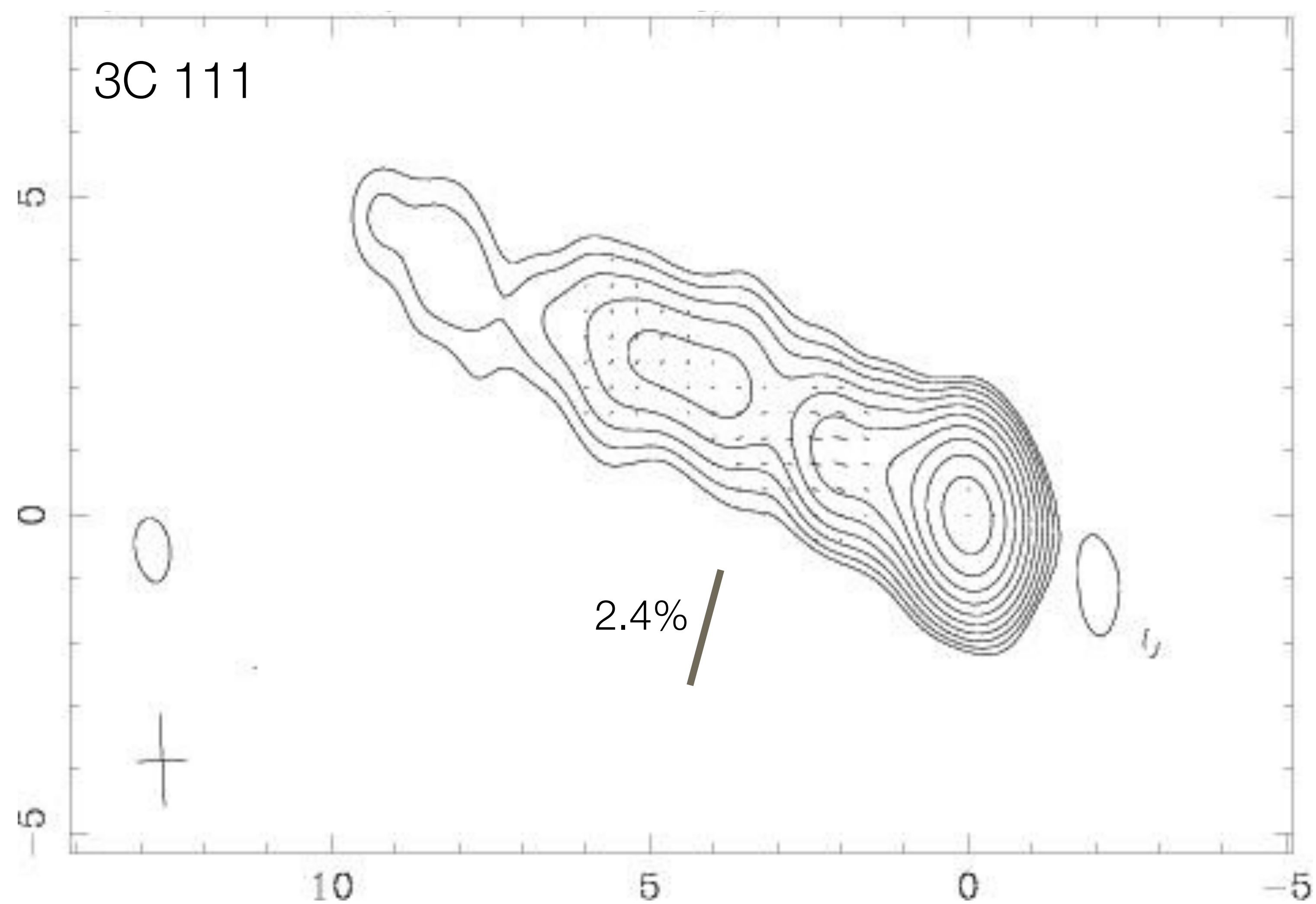

Results

EVPA swings

PKS 1510-089

Radiative "swing"

Shows all characteristics of the signature

Multi-band data help the interpretation

Paces:

1st rotation:

1.2°/day (5 GHz)

0.5°/day (10 GHz)

2nd rotation:

1.2°/day (5 GHz)

0.8°/day (10 GHz)

Difficult to explain with geometrical swing scenario

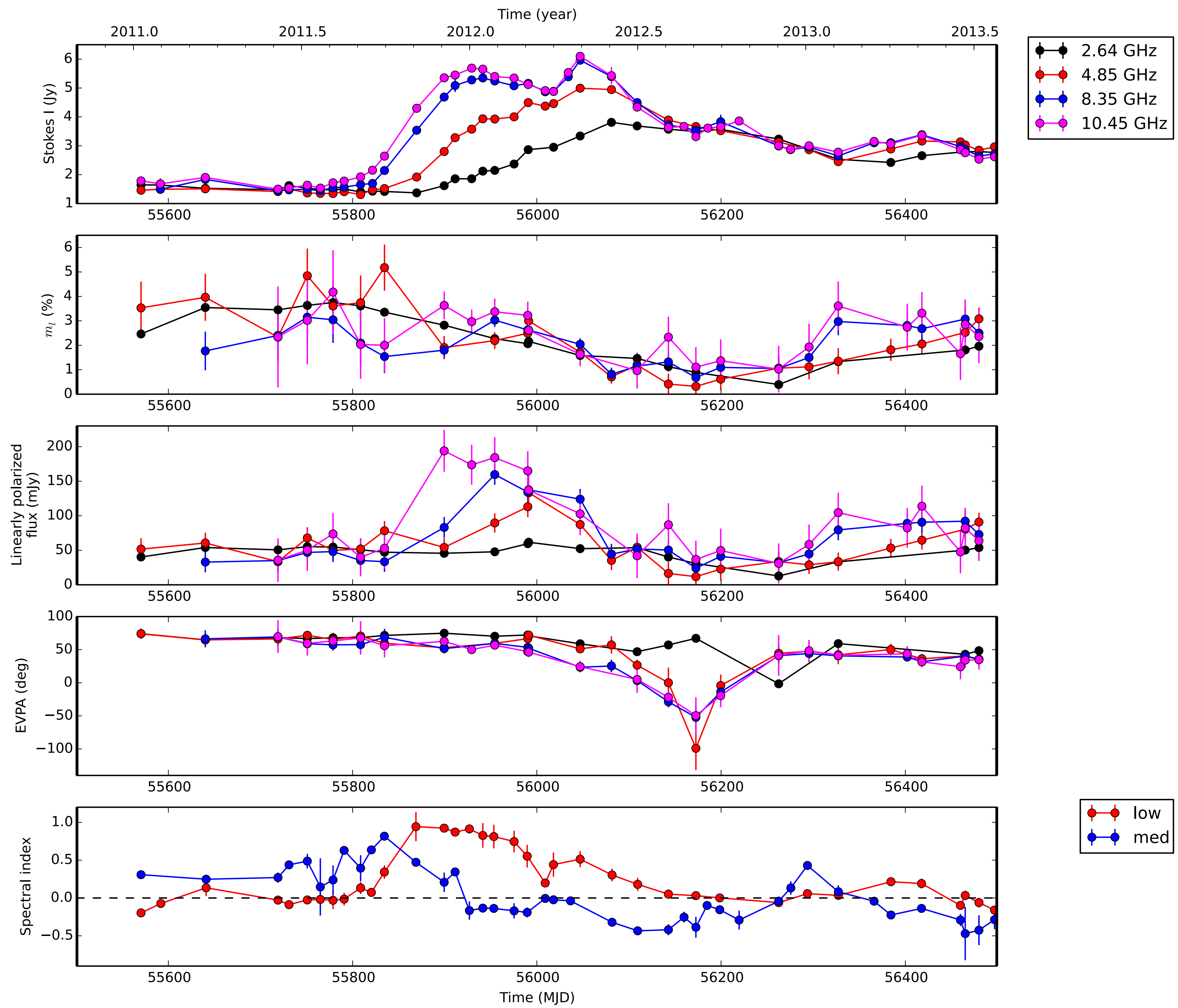

Myserlis et al. (2014)

Results

EVPA swings

J1849+6705

Geometrical swing

~175 degrees

Multi-band data help the interpretation

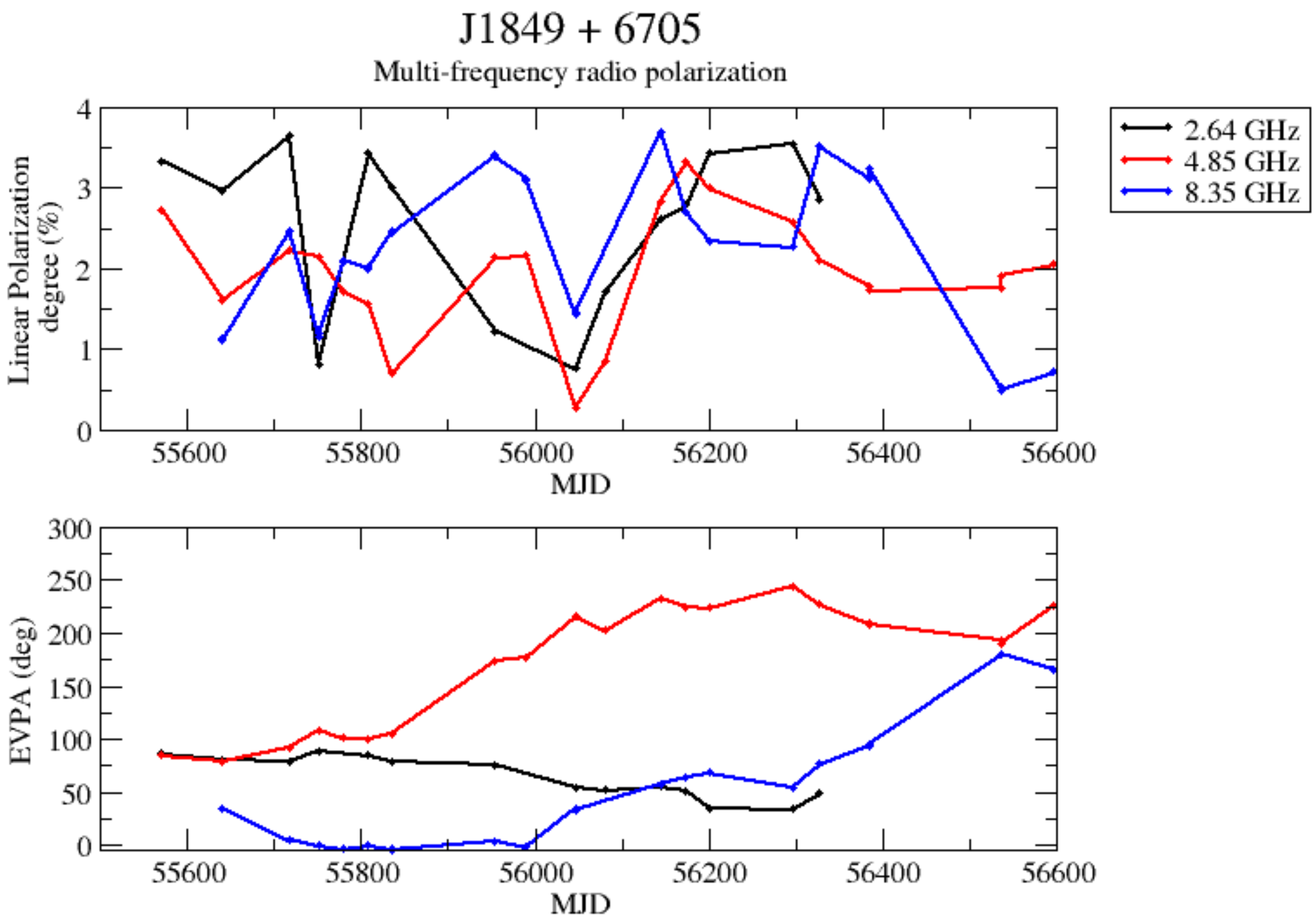

Summary

- Multi-frequency linear and circular radio polarization monitoring data are invaluable for the investigation of the AGN jet physics
  - B-field magnitude
  - B-field uniformity / topology
  - Pitch angle distribution
  - Jet plasma state
  - Jet plasma composition

Summary

- Multi-frequency high-cadence monitoring programs
    - F-GAMMA program
- Data reduction techniques and caveats
- Results
    - CP calibrators
    - B-field magnitude
    - EVPA vs jet orientation
    - EVPA swings: Geometrical & Radiative